NUWC-NPT Technical Report 12,360
27 November 2020

Loggerhead Sea Turtle Density in the Mediterranean Sea

Laura M. Sparks
NUWC Division Newport

Andrew D. DiMatteo
McLaughlin Research Corporation

NEWPORT

Naval Undersea Warfare Center Division Newport, Rhode Island

PREFACE

This report was prepared under NUWC Division Newport Network Activity No. 100001483098 0010, “Density Modeling for Loggerhead Sea Turtles in the Mediterranean Sea,” principal investigator Laura M. Sparks (Code 1023). The sponsoring activity is the U.S. Fleet Forces Command, program manager Laura Busch (USFF N465).

The technical reviewer for this report was Tara E. Moll (Code 1023).

The authors would like to thank all the data providers and organizations that contributed line transect surveys and dive data to this project: Blue World Institute, The University of Valencia, Tethys Institute, ISPRA, IFAW, The University of Exeter, ACCOBAMS, PELAGIS, Alnitak, Stazione Zoologica Anton Dorne, Julie Belmont, Simone Panigada, Olivier Boisseau, Giancarlo Lauriano, Drasko Holcer, Caterina Fortuna, Vincent Ridoux, Helene Peltier, Toni Raga, David March, Robin Snape, Sandra Hochscheid, Annette Broderick, Brendan Godley, Robin Snape, and Julia Haywood. Jason Roberts and Ana Canadas provided analytical support and cleaned and delivered much of the line transect survey data. Elizabeth Becker and David Miller provided R code and advice on including environmental variability in the uncertainty estimate. Danielle Jones of the Naval Facilities Engineering Command Atlantic assisted with project management.

Reviewed and Approved: 27 November 2020

Dennis J. Tierney
Head, Infrastructure Division

REPORT DOCUMENTATION PAGE	*Form Approved* *OMB No. 0704-0188*

1. REPORT DATE (*DD-MM-YYYY*)	**2. REPORT TYPE**	**3. DATES COVERED (*From – To*)**
27-11-2020	Technical Report	1 FEB 2019 to 31 APR 2020

4. TITLE AND SUBTITLE Loggerhead Sea Turtle Density in the Mediterranean Sea	**5a. CONTRACT NUMBER** **5b. GRANT NUMBER** **5c. PROGRAM ELEMENT NUMBER**
6. AUTHOR(S) Andrew D. DiMatteo and Laura M. Sparks	**5d. PROJECT NUMBER** **5e. TASK NUMBER** **5f. WORK UNIT NUMBER**
7. PERFORMING ORGANIZATION NAME(S) AND ADDRESS(ES) Naval Undersea Warfare Center Division 1176 Howell Street Newport, RI 02841-1708	**8. PERFORMING ORGANIZATION REPORT NUMBER** TR 12,360
9. SPONSORING/MONITORING AGENCY NAME(S) AND ADDRESS(ES) U.S. Fleet Forces Command 1562 Mitscher Ave Norfolk, VA 23551	**10. SPONSORING/MONITOR'S ACRONYM** USFF **11. SPONSORING/MONITORING REPORT NUMBER**

12. DISTRIBUTION/AVAILABILITY STATEMENT
DISTRIBUTION STATEMENT A: Approved for public release; distribution is unlimited.

13. SUPPLEMENTARY NOTES

14. ABSTRACT. Loggerhead turtles are a globally vulnerable species of marine turtle. The Mediterranean Sea subpopulation, which ranges throughout the entire Mediterranean basin, is listed as least concern but experiences significant threats in the region including bycatch in fisheries, climate change, coastal development, and marine pollution. Broad-scale patterns of distribution and abundance can provide regional managers a tool to effectively conserve and manage this species at basin and sub-basin scales. Here NUWC uses aerial and shipboard line transect survey data collected between 2003 and 2018 to estimate density and abundance throughout the Mediterranean Sea using distance sampling methodology. A spatial density model estimating loggerhead density, abundance, and distribution across the Mediterranean Sea was generated as a long-term annual average. The model was adjusted for availability bias using dive data from loggerhead turtles tagged with time depth recorders from multiple regions within the Mediterranean Sea. Geographic extrapolation in areas near surveys was undertaken with caution. Mean abundance for the long-term average model was estimated as 994,000 (CV 0.20). This estimate represents the first basin-wide estimate of abundance for this species in the Mediterranean not based on demographic models.

15. SUBJECT TERMS
Loggerhead Sea Turtles, Mediterranean, Distance Sampling, Density, Navy Marine Species Density Database

16. SECURITY CLASSIFICATION OF:			**17. LIMITATION OF ABSTRACT**	**18. NUMBER OF PAGES**	**19a. NAME OF RESPONSIBLE PERSON**
a. REPORT	**b. ABSTRACT**	**c. THIS PAGE**			Laura M. Sparks
U	U	U	SAR	77	**19b. TELEPHONE NUMBER** *(Include area code)* (401) 832-7019

(Next page blank)

TABLE OF CONTENTS

LIST OF ILLUSTRATIONS

LIST OF TABLES

LIST OF ABBREVIATIONS AND ACRONYMS

ACCOBAMS	Agreement for the Conservation of Cetaceans of the Black Sea, Mediterranean Sea, and Contiguous Atlantic Area
AIC	Akaike Information Criteria
ASI	ACCOBAMS Survey Initiative
BWI ISPRA	Blue World Institute and Italian Institute for Environmental Protection and Research
CI	Confidence Interval
CV	Coefficient of Variation
EEZ	Exclusive Economic Zone
ESA	Endangered Species Act
GAM	Generalized Additive Model
GPS	Global Positioning System
IFAW	International Fund for Animal Welfare
IUCN	International Union for the Conservation of Nature
MCR	Marine Conservation Research
MMPA	Marine Mammal Protection Act
NEMO	Nucleus for European Modeling of the Ocean
NMSDD	Navy Marine Species Density Database
NUWC	Naval Undersea Warfare Center
PELAGIS	Systèmes d’Observation pour la Conservation des Mammifères et Oiseaux Marins
Q-Q	Quantile-Quantile
REML	Relative Maximum Likelihood
SRTM	Shuttle Radar Topography Mission
TETHYS	Tethys Institute
U.S.	United States
VGPM	Vertically Generalized Production Model

LOGGERHEAD SEA TURTLE DENSITY IN THE MEDITERRANEAN SEA

1. INTRODUCTION

The United States (U.S.) Department of the Navy requires spatially explicit estimates of species distribution and abundance to assess the impacts associated with training and testing activities in the Mediterranean Sea. To conduct this analysis, the Navy compiles density and abundance estimates in the Navy Marine Species Density Database (NMSDD), which is the authoritative source of marine species density data for the Navy.

In the Mediterranean Sea, the Navy is active at several installations, both U.S. and foreign owned (figure 1), and training and testing occurs at both the unit level and in conjunction with the navies of other nations. The U.S. Navy conducts risk assessments to evaluate impacts to marine species on a per exercise basis, which assess the potential for negative interactions between Navy assets using sonar and explosives and protected marine species prior to conducting training and testing activities.

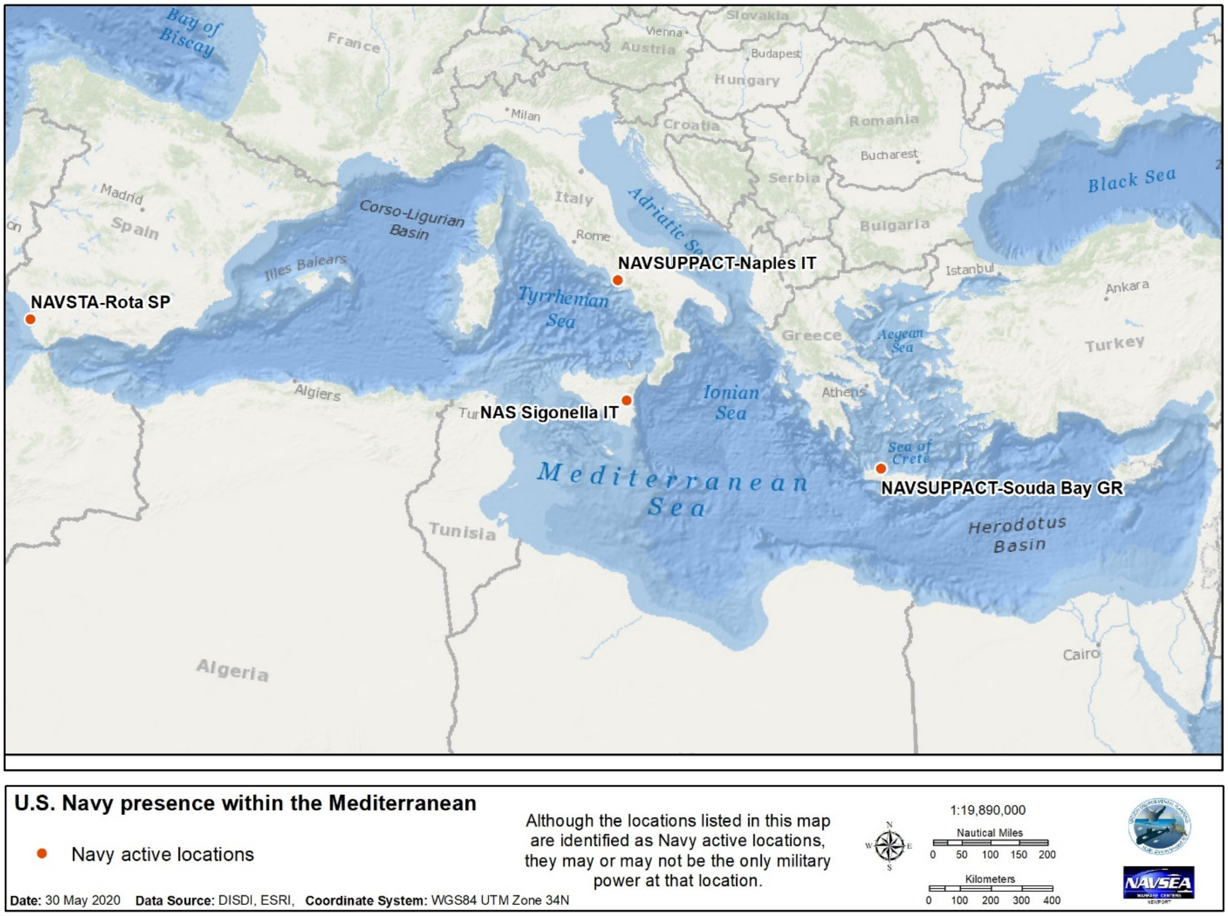

Figure 1. Navy Active Locations in the Mediterranean Sea

Risk assessments consider marine species listed under U.S. domestic law, the Endangered Species Act (ESA) and the Marine Mammal Protection Act (MMPA), and the International Union for the Conservation of Nature's (IUCN) Red List of Threatened Species. Risk assessments consider the number of U.S. platforms using sonar or explosives, the type of sonar (frequency and source level), visibility, probability of surface ducting, habitat structure, potential for limited egress, and animal presence. The Navy uses density models as the best available science for estimating abundance and distribution of these species in the Mediterranean Sea.

The Navy requires density data used in permitting and risk assessments to predict absolute density/abundance of animals, have a spatial resolution of 10 kilometers (6.2 miles) or less where possible, represent a long-term average of density/abundance, and have the finest scale temporal and taxonomic resolution scientifically supportable. The models are generally derived from line transect data, both aerial and shipboard, and relate animal presence to environmental covariates. This allows animal density to vary in response to the underlying environmental conditions. Other data types, such as satellite telemetry data coupled with a population estimate, can be used, but these alternate data types are less preferable.

Previous work funded by the Navy produced spatial density models for eight taxa of marine mammals in the Mediterranean Sea, but the Navy has not produced models for the two extant species of sea turtles, loggerhead (*Caretta caretta*) and green (*Chelonia mydas*), that nest in the Mediterranean Sea. This report partially fills that gap by developing a spatial density model for loggerhead sea turtles in the Mediterranean Sea.

The Naval Undersea Warfare Center (NUWC) Division, Newport, RI, followed the general approach to fitting spatial density models outlined by Miller (2013) and included an extrapolation assessment similar to Mannocci et al. (2018a) to assess the amount of spatial, temporal, and environmental extrapolation that occurred. NUWC was also able to include estimates of availability bias that were stratified spatially and temporally.

2. BACKGROUND

2.1 THE MEDITERRANEAN SEA

The Mediterranean Sea is a large, semi-enclosed body of water, located between southern Europe and Northern Africa. It is connected to the Atlantic Ocean by the Strait of Gibraltar, to the Black Sea by the Bosphorus Strait, and to the Red Sea by the Suez Canal. Connected to the Mediterranean are several other semi-isolated water bodies that NUWC included as part of the Study Area; the Adriatic Sea, the Aegean Sea, and the Ionian Sea—that will referred to collectively as the Mediterranean Sea for the sake of convenience.

The Mediterranean Sea is characterized by narrow continental shelves, steep slopes, and extensive abyssal plains. It includes many bathymetric features known to influence the distribution of marine megafauna, such as submarine canyons and hundreds of seamounts (Mussi et al. 2014, Tepsich et al. 2014, and Fiori et al. 2014). The waters of the Mediterranean Sea are generally salty and nutrient-poor (Longhurst 2007), due in part to its enclosed nature.

Water temperature and primary productivity move in seasonal cycles in the Mediterranean Sea, driven by insolation, inflow from the Atlantic Ocean and major rivers in the eastern Mediterranean Sea, and wind stress. Winter is characterized by lower sea surface temperatures but higher productivity, and summer has higher sea surface temperatures and lower productivity. In general, productivity is higher in the western Mediterranean Sea than the Eastern Mediterranean Sea (Lazzari et al. 2012). The two major basins are separated by an undersea ridge system between the island of Sicily and the Tunisian/Libyan coast.

2.2 SEA TURTLES IN THE MEDITERRANEAN SEA

There are seven extant species of sea turtles globally, all listed as vulnerable, threatened, or endangered by the IUCN, except for the flatback turtle (*Natator depressus*) that is listed as data deficient (Marine Turtle Specialist Group 2020). In the Mediterranean Sea, two species of sea turtles, the loggerhead and green are resident, in that they have nesting colonies within the Mediterranean Sea (Wallace et al. 2010). Other species of sea turtles, including leatherback (*Dermochelys coriacea*), Kemp's ridley (*Lepidochelys kempii*), and olive ridley (*Lepidochelys olivacea*), are periodically sighted in the Western Mediterranean Sea, having migrated into the basin via the Strait of Gibraltar (Casale et al. 2003, Tomás and Raga 2008, Carreras et al. 2014 and Revuelta et al. 2015). However, they are considered infrequent visitors to the region.

The Mediterranean loggerhead population is listed as least concern by the IUCN, though the species is globally listed as vulnerable (Casale 2015, and Casale and Tucker 2017). Green turtles are listed as endangered globally by the IUCN (Seminoff 2004). No regional assessment for the Mediterranean has been made for green turtles.

The primary nesting sites for loggerhead sea turtles in the Mediterranean Sea are found along the coasts of Greece, Turkey, Cyprus, and Libya (Casale and Margaritoulis 2010), although loggerhead nesting sites can be found elsewhere in the Eastern Mediterranean in lower concentrations. In the Western Mediterranean, loggerhead nesting is much more sporadic, but limited nesting does occur in Spain, France, and Italy (Casale and Margaritoulis 2010).

Green turtle nesting is more strictly limited to the Eastern Mediterranean, and major rookeries are found in Turkey, Cyprus, and Syria, with more limited nesting in Egypt, Lebanon, and Israel (Casale and Margaritoulis 2010). There are far fewer green turtles than loggerheads nesting in the Mediterranean. Estimates of adult female populations are approximately 15,000 for loggerheads and approximately 4,000 for green turtles in the entire Mediterranean Sea (Casale and Heppell 2016), although this is likely an underestimate given the lack of comprehensive surveys of all potential nesting habitat. The best demographic estimates for the resident populations, including pelagic juveniles, range from 0.8 to 3.4 million for loggerheads and 176,000 to 2.2 million for green turtles. The loggerhead estimate does not include pelagic juveniles of Atlantic origin.

Juveniles of both species are largely pelagic, recruiting to neritic foraging areas as sub-adults (Casale and Marini 2014, Carreras et al. 2006, Clusa et al. 2014, Cardona and Hays 2018, Snape et al. 2016 and Casale et al. 2018). Green turtle distribution is limited to the Eastern Mediterranean (figure 2), while loggerheads range throughout the entire basin (Wallace et al. 2010). In the Western Mediterranean, pelagic loggerheads from multiple populations mix (figure 2). Juveniles from the Northwest and Northeast Atlantic populations entrain in the Mediterranean, entering via the Strait of Gibraltar, and they stay for as many as ten years (Eckert et al. 2008, Revelles et al. 2008, and Clusa et al. 2014). The proportion of juvenile loggerheads of Atlantic origin can be higher than 30 percent in some areas (Carreras et al. 2006 and 2011). Because of this mixing, demographic modeling alone is not enough to estimate the full population of loggerhead sea turtles in the Mediterranean Sea.

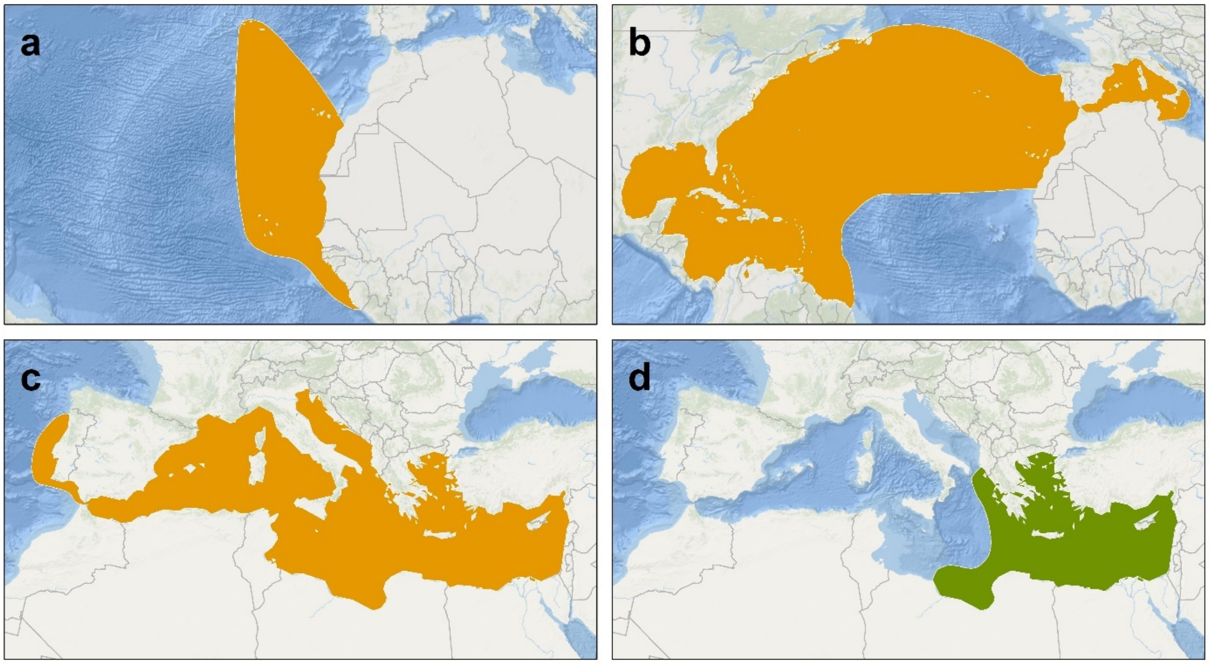

Figure 2. Primary Range of Sea Turtle Populations in the Mediterranean Sea

Note: In figure 2, the Regional Management Units show the primary range of populations of sea turtles found in the Mediterranean Sea (Wallace et al. 2011). (a) Northeast Atlantic Loggerheads, (b) Northwest Atlantic Loggerheads, (c) Mediterranean Loggerheads, and (d) Mediterranean Greens.

The following section describes the methods used to generate spatial density models for loggerhead sea turtles of all age classes and origins present in the Mediterranean Sea. Models for green turtles were not attempted because there was limited survey coverage in the Eastern Mediterranean, where they are distributed. This, coupled with their lower population, led to too few confirmed sightings to fit a spatial density model or discriminate unidentified hardshell turtle sightings using machine learning methods as done by Roberts et al. (2018).

This study builds off previous work performed by the Marine Spatial Ecology Lab at Duke University, which was funded by the U.S. Navy (Roberts et al. 2018 and Mannocci et al. 2018b). This previous work collected line transect survey data from multiple organizations in the Mediterranean Sea that were appropriate for inclusion in a density modeling framework, established a workflow for producing density models, and predicted density and associated uncertainty for several taxa of marine mammals in the Mediterranean Sea.

NUWC reached out to these same organizations to request their permission to use the data gathered and prepared by Duke for this follow-on effort modeling loggerhead density. NUWC generally followed the modeling framework previously used by Duke with some methodological improvements detailed in the following sections. NUWC believes that this is appropriate given that loggerhead turtles are a wide ranging, diving marine taxa, like marine mammals. Appropriate adjustments for sea turtle ecology and life history were made where appropriate. The resulting loggerhead density model is methodologically consistent with models previously funded by the Navy and is the first basin-wide loggerhead density model for the Mediterranean Sea.

3. MATERIALS AND METHODS

3.1 STUDY AREA

The Study Area for this project (e.g., the area over which density predictions were made) was the same as that established by Mannocci et al. (2018b). The authors of that study worked with the Navy to delineate an appropriate study area for marine mammal models in the Mediterranean Sea that covered biologically important areas for marine mammals and areas that were of interest to the Navy.

This study area eliminated many inland waters that would be difficult to model due to poor performance of remotely sensed covariates close to shore and that were not covered by surveys. Given the cosmopolitan distribution of loggerhead sea turtles in the Mediterranean Sea and our model sharing many candidate covariates with previous marine mammal models, NUWC felt that using the same study area was appropriate. This also promoted consistency with density data already included in the NMSDD, the Navy's repository for spatial density models for protected species.

NUWC was able to successfully fit a spatial density model to all portions of the Study Area. No areas contain stratified estimates derived from the literature or extrapolation of values taken from another area, though other forms of extrapolation are present (see section 3.5.2).

3.2 SURVEY DATA PROCESSING AND INGESTION

Previous gap analyses and Navy-funded modeling efforts identified over 300,000 km (186,411 mi) of line transect surveys in the Mediterranean from 2003 to 2016 that were appropriate for inclusion in density spatial modeling efforts (Mannocci et al. 2018a, 2018b). These surveys came from 12 different organizations and spanned most regions within the Mediterranean Sea. Seven of them were willing to contribute their data to the creation of Navy-funded marine mammal spatial density models.

The Duke University modeling team took these data and ensured that they contained all the requisite components to perform distance sampling; time, location, species, group size, and perpendicular distance to the animal(s) from the trackline (Buckland et al. 2001), which is a prerequisite for spatial density models. Most collaborators also included sighting and survey level covariates, such as sea state or weather conditions, that might influence the probability of sighting an animal and, therefore, the detection functions.

The Duke team split the on effort portions of the shared survey data into 5-km (3-mi) segments, the same resolution as the finest scale candidate covariates for the spatial density model. Abundance was predicted for each of these segments, which then formed the response variable for the subsequent spatial density model. Not all transects could be split into perfectly even 5-km (3-mi) segments, so the Duke team developed an algorithm to split the segments as close to 5-km (3-mi) as possible (Mannocci et al. 2018b). The exception was the Alnitak/Alnilam shipboard surveys, which had pre-made segments that the Duke modeling team opted to use.

All seven organizations that shared survey and sightings data with the Duke team for the marine mammal models also shared sea turtle sightings, though Duke was not contracted to produce any sea turtle models. NUWC reached out to these organizations and received permission to use these data to create a loggerhead spatial density model for the Mediterranean Sea.

One set of surveys from EcoOcean did not include perpendicular distances for their sea turtle sightings and, therefore, were not included in the NUWC model. The Duke team shared the already processed survey data and sightings from the other six organizations. NUWC then reviewed the sightings data for quality control purposes and linked them to the survey data segments. Section 4.1 has more detail on quality control of sightings for individual survey programs. See Mannocci et al. (2018b) for more details on how survey transects were processed into segments.

In addition to the data provided by the Duke team, there was a survey in the summer of 2018 that covered almost the entire Mediterranean Sea using both aerial and shipboard platforms. The survey was performed under the Agreement for the Conservation of Cetaceans of the Black Sea, Mediterranean Sea, and Contiguous Atlantic Area (ACCOBAMS). NUWC received permission to use these data in their model.

NUWC split the ACCOBAMS shipboard survey data into segments using the methods laid out in Mannocci et al. (2018b) and linked sightings to segments. The ACCOBAMS aerial surveys did not collect perpendicular distances to turtle sightings, which normally would exclude them from use in distance sampling analyses. After discussion with data providers and regional experts, NUWC decided that it would be reasonable to treat the ACCOBAMS aerial survey line transects as strip transects that allowed them to be incorporated into the modeling framework. They subsequently split the ACCOBAMS aerial survey transects into 5-km (3-mi) segments and linked segments to sightings as was done with the surveys that included perpendicular distances. More details on how these data were treated can be found in the subsequent sections.

3.3 SURVEY DATA SUMMARY

3.3.1 Overview of Effort Data

NUWC received permission to use data from eight different organizations, seven of which were usable in a distance-sampling framework. Line transect surveys from those eight organizations covered 229,598 linear km (142,666 linear mi) of effort, split between 56,171 km (34,903 mi) of shipboard surveys and 173,427 km (107,763 mi) of aerial surveys (table 1). These surveys occurred from 2003 to 2018 and covered all seasons, though there are major differences in survey coverage between months. There were data from Alnitak/Alnilam surveys that occurred during the 1990s, but NUWC opted to drop these data from the analysis (see section 4.1).

Table 1. Summary of Survey Effort and Sightings

Survey	Platform	Region	Years	Effort (linear km)	Useable sightings	Group size >1	Notes
ASI	aerial	All subregions	2018	55,498	3745	5%	All given as hardshell, several hundred sightings in eastern Mediterranean
BWI ISPRA	aerial	Adriatic Sea	2010, 2013	16,595	2010	2%	All given as hardshell
PELAGIS	aerial	Algero-Provençal basin, Tyrrhenian Sea/eastern Ligurian Sea	2011, 2012	32,240	371	2%	All given as hardshell
TETHYS ISPRA	aerial	Algero-Provençal basin, Tyrrhenian Sea/eastern Ligurian Sea, Ionian Sea	2009–2011, 2013, 2014, 2016	61,996	5792	6%	All given as hardshell
University of Valencia	aerial	Algero-Provençal Basin	2010, 2011, 2013	7,098	81	2%	All loggerhead
Alnitak/ Alnilam	shipboard	Alborán Sea/Strait of Gibraltar	1999-2011	42,094	441	7%	All loggerhead
Song of the Whale (IFAW/MCR)	shipboard	All subregions but the Adriatic Sea	2003, 2004, 2005, 2007, 2013	7,013	64	5%	62 hardshell, 2 confirmed loggerhead
Song of the Whale (ASI)	shipboard	Alborán Sea/Strait of Gibraltar, Algero-Provençal Basin, Tyrrhenian Sea/eastern Ligurian Sea, Strait of Sicily/Tunisian Plateau/Gulf of Sirte, and Ionian Sea/Central Mediterranean	2018	7,064	98	6%	31 hardshell, 67 confirmed loggerhead
TOTALS				229,598	12,602		

ASI = ACCOBAMS Survey Initiative
BWI ISPRA = Blue World Institute and Italian Institute for Environmental Protection and Research
PELAGIS = Systèmes d'Observation pour la Conservation des Mammifères et Oiseaux Marins
TETHYS = Tethys Institute
IFAW = International Fund for Animal Welfare
MCR = Marine Conservation Research

Surveys covered all major regions within the Mediterranean Sea, but coverage was sparse in the Eastern Mediterranean and absent in a few Southern areas. Figure 3 shows the geographic coverage of incorporated surveys and associated sightings. Figures of survey effort segregated by month are in the appendix. Figure 4 shows regions referenced in this study.

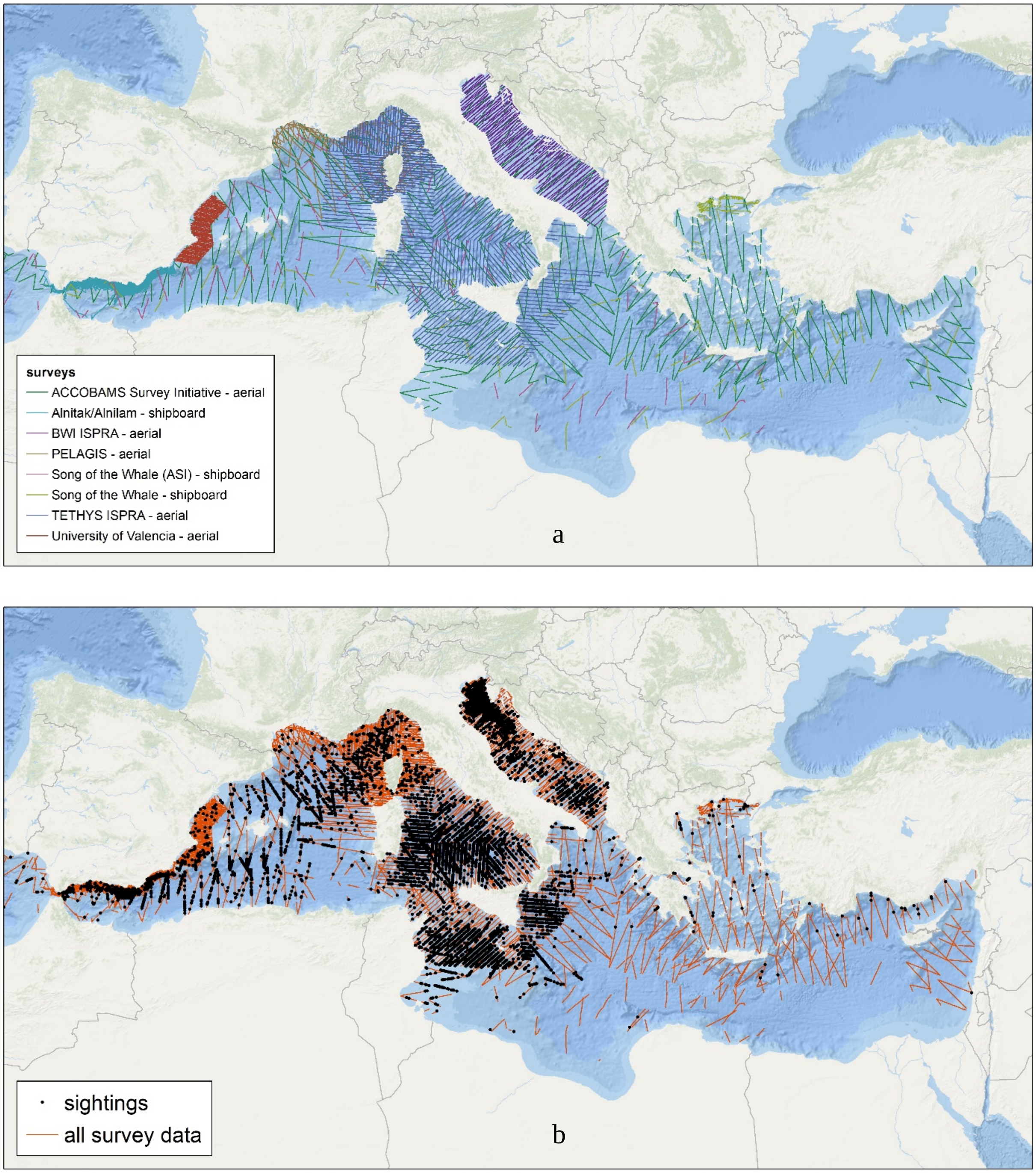

Figure 3. Survey Coverage by Organization (a) and with Sightings Overlaid (b)

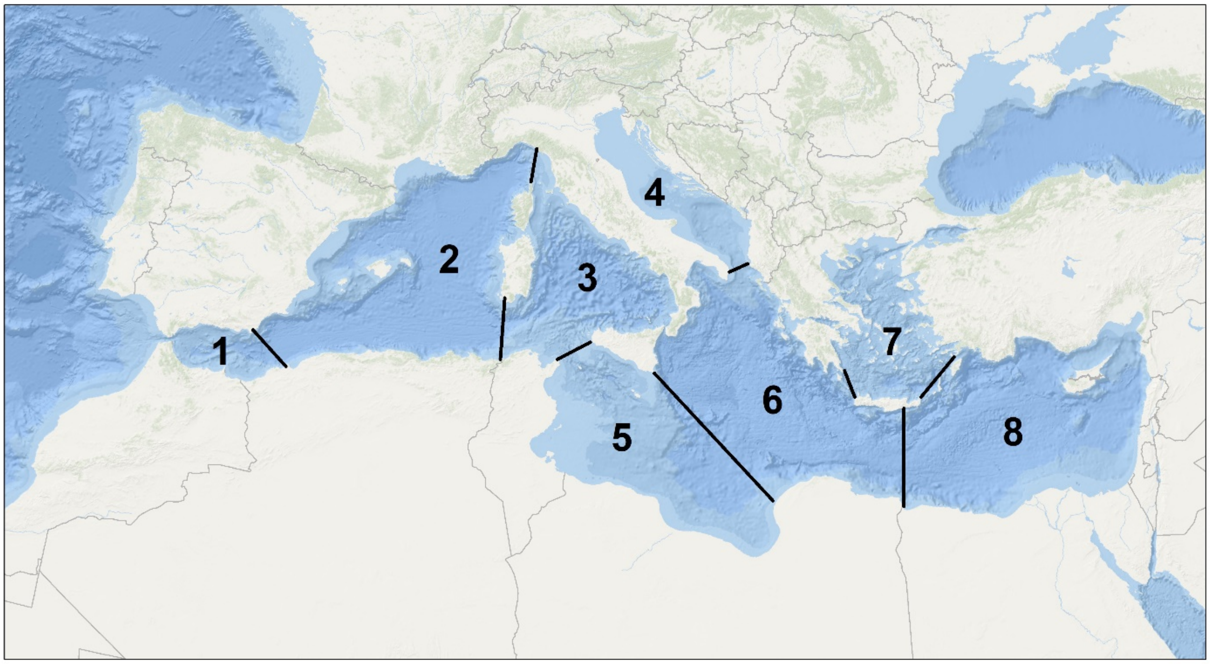

Figure 4. Designated Sub-Areas of the Mediterranean Sea

Note: In figure 4: (1) Alborán Sea/Strait of Gibraltar, (2) Algero-Provençal Basin, (3) Tyrrhenian Sea/Eastern Ligurian Sea, (4) Adriatic Sea, (5) Strait of Sicily/Tunisian Plateau/Gulf of Sirte, (6) Ionian Sea/Central Mediterranean, (7) Aegean Sea, and (8) Levantine Sea. Throughout this document, references to the Eastern Mediterranean, refer to (6) and (8) Combined.

3.3.2 Overview of Sightings Data

Sightings for marine turtles in the available survey data were given as either loggerhead, green, leatherback, or an unidentified hardshell turtle. There was only one confirmed leatherback sighting and less than ten confirmed green turtle sightings.

NUWC used all confirmed loggerhead sightings as well as unidentified hardshell turtle sightings in the model. This decision was made because green turtles are limited to the Eastern Mediterranean, other hardshell turtle species are rare, and unidentified sightings could reasonably be assumed to be mostly loggerhead sea turtles.

The BWI ISPRA survey located in the Adriatic Sea gave all sightings as hardshell turtles, but NUWC can assume that the majority were loggerheads based on previous studies (Fortuna et al. 2015). TETHYS ISPRA and PELAGIS observations were given as hardshell turtles but can all be assumed to be loggerheads given their location in the north-Central Mediterranean. Most shipboard survey sightings were unidentified, but because of the low coverage in the Eastern

Mediterranean, most can be assumed to be loggerheads. The ASI aerial surveys had the most sightings in the Eastern Mediterranean of any survey and reported all sightings as unidentified hardshell turtles. Because this is where green turtles can be found, it is likely that some of the ASI aerial survey sightings are of green turtles.

There were too few confirmed sightings of green turtles (less than 10) to attempt to use machine learning to assign unidentified turtles to be either green or loggerhead sea turtles. The likely inclusion of green turtles in some of the surveys that cover the Eastern Mediterranean is a source of overestimation of the number of loggerheads in the Eastern Mediterranean (treating green turtles as loggerheads). A more detailed discussion of possible sources of over- and under-estimation can be found in section 5.

Some sightings were dropped because they were missing detection function covariates or perpendicular distances. Any survey segments with dropped sightings were dropped from all subsequent analyses. This generally amounted to less than two percent of the segments of any given survey.

Group size was predominately one, though larger groups were detected. Groups larger than one accounted for two to seven percent of sightings depending on the survey, and the largest group size detected was 10. Aside from mating aggregations, sea turtles are generally solitary (Bolten 2003), so this trend was unsurprising. Table 1 has a summary of sightings by survey and percent of sightings with a group size greater than one.

3.4 DETECTION MODELING

3.4.1 General Approach to Detection Function Fitting

The first step in spatial density modeling, after preparing survey data and sightings, is to model detectability by fitting detection functions. Detection functions are derived from perpendicular distances and, in some cases, associated covariates. Histograms of perpendicular distances were generated for each survey to explore the need for truncation. Buckland et al. (2011) recommend that distant sightings are truncated (right truncation) to maintain a minimum probability of detection of 0.15. Left truncation, e.g., removing sightings near the trackline, is generally only used in special circumstances and was only necessary here for one survey (see section 3.4.2).

The ability to sight animals generally varies by survey platform and protocol. As such, it is desirable to fit separate detection functions by platform and survey if there are enough sightings to meet the recommended 60 sightings threshold for fitting robust detection functions (Buckland et al. 2011). While this threshold is not a hard and fast rule, detection functions with fewer sightings can be less robust, and it can be difficult to include covariates in the model.

All surveys had more than the recommended 60 sightings, so no pooling was required between surveys or platforms. NUWC pooled multiple years of the same survey program in order to be able to fit more complex detection functions, unless there was good reason not to pool. All surveys had associated survey condition covariates (table 2) that allowed NUWC to attempt multi-covariate distance sampling (Marques and Buckland 2004).

Table 2. Survey Platform Height, Speed, and Covariates Collected

Survey	Platform	Altitude (m)	Mean speed (knots)	Covariates collected
PELAGIS	Britten Norman aircraft with bubble windows	183	90	Beaufort sea state, cloud cover, glare, turbidity, subjective conditions
TETHYS ISPRA	Partenavia P-68 aircraft with bubble windows	213	100	Beaufort sea state, cloud cover, glare, turbidity, subjective conditions
BWI ISPRA	Partenavia P-68 aircraft with bubble windows	198	100	Beaufort sea state, cloud cover, glare, turbidity, subjective conditions
University of Valencia	Cessna 337 aircraft with flat windows	152 (2010, 2011); 213 (2013)	90	Beaufort sea state, visibility
Alnitak/Alnilam	18 m motor sailboat R/V Toftevaag	3.5 (deck); 11 (mast)	4.5	Douglas sea state, swell, sight ability
IFAW/MRC	Motor sailboats with 21 and 14 m lengths	5.3	6.5	Beaufort sea state, cloud cover, glare, swell, wave height, visibility
ASI shipboard	Motor sailboats with 21 and 14 m lengths	5.3	6.5	Beaufort sea state, cloud cover, glare, swell, wave height, visibility
The ASI aerial surveys used a strip transect methodology and so are not included in this table.				

All combinations of survey condition covariates were attempted for both half-normal and hazard rate functions, which are the two most common base functions for detection functions. Other tested covariates included year (for surveys with multiple years), month, and observer position. Group size was not included as a covariate because there was little variation in group size. Ordinal variables such as Beaufort sea state were also tested as factors. The two base functions–hazard rate and half-normal–were also tested on their own and with cosine adjustments.

Model selection was based on Akaike Information Criteria (AIC), which is used to assess the trade-off between goodness of fit and model simplicity. NUWC selected the model with the lowest AIC. If more than one best model had similar AIC (within 2), NUWC would choose between them based on goodness of fit statistics. For all selected models, NUWC examined quantile-quantile (Q-Q) plots, detection plots, and goodness of fit statistics to make sure models were reasonable.

3.4.2 Special Cases

3.4.2.1 Alnitak/Alnilam shipboard surveys. The pre-2006 Alnitak/Alnilam surveys were missing perpendicular distance data. Previously, analyses of these data made assumptions about the detectability of these sightings based on similar segments from later surveys (Cañadas pers. comm. 2019). NUWC decided to drop the pre-2006 data rather than extrapolate the detection function because there were still more than 60 sightings in the post-2006 data to fit detection functions and this area was well covered by both the ASI aerial surveys and various Song of the Whale surveys in later years.

The Alnitak/Alnilam surveys also had detections from two platforms of different heights (table 2). Ideally, different detection functions would have been fit to each of these platforms. However, there were too few sightings from the mast to fit a reasonable detection function on its own. This was true even if the pre-2006 sightings were included. Because of this, the two sets of sightings were combined and observer position was included as a potential covariate in the detection function.

3.4.2.2 ASI aerial survey. The ASI aerial survey did not record perpendicular distances to sea turtles. They adopted a strip transect approach for sea turtles and seabirds. Discussing with the survey data providers, they assumed all sea turtles and seabirds within a 200-meter (656 feet) strip on either side of the plane were detected (Panigada and Cañadas pers. comm. 2019). With a strip transect methodology, no detection function is fitted, so no additional covariates are used. Density per segment is calculated by dividing the number of individuals sighted by the area covered.

3.4.2.3 University of Valencia aerial surveys. The University of Valencia aerial surveys occurred at different heights in different years (table 2). That can affect detection distance and detectability. NUWC attempted to fit different detection functions to these years, but the resulting detection functions were not satisfactory. The Q-Q plots were skewed, and no covariates were able to be fit because there were too few sightings. Because of this, the decision was made to combine all years of the surveys to fit a detection function and include year as a potential covariate.

These surveys were also performed in an aircraft with flat windows, limiting visibility of the trackline. A histogram of observations versus distance (figure 5) shows sightings dropping off close to the trackline. This causes problems in fitting the detection function because a core assumption of distance sampling is that all animals on the trackline are detected. While not desirable, this is a special circumstance where left truncation is merited. The left truncation distance of 104 m (341 ft) previously reported by the Duke team in Mannocci et al. (2018b) was used.

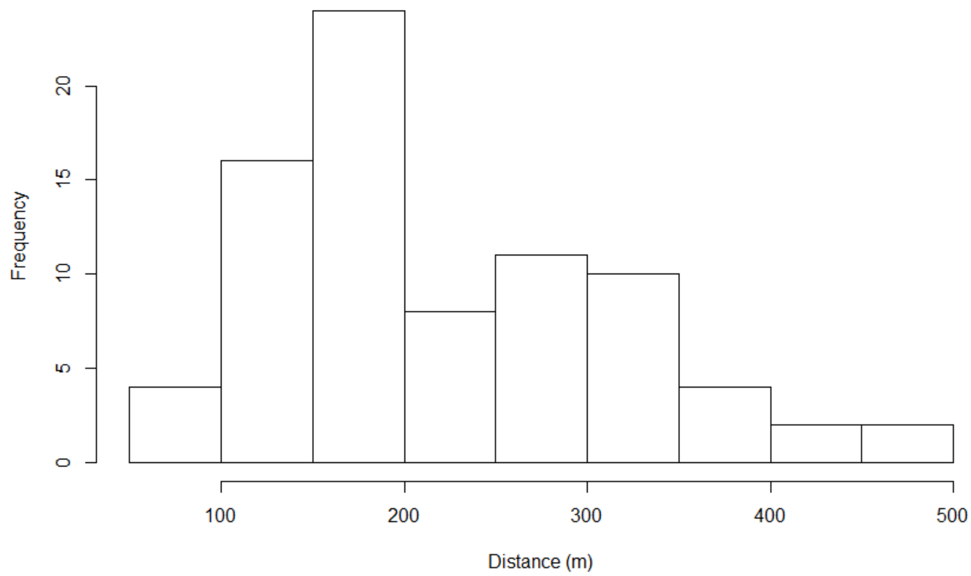

Figure 5. University of Valencia Pooled Aerial Survey Observations versus Perpendicular Distance

Lastly, there was one sighting where the reported group size was 18. NUWC felt this was erroneous and confirmed with the original data providers that this was likely a typo and should be changed to a group size of one. The second largest group size for any other survey was 10.

3.4.3 g(0) Correction for Availability and Perception Bias

The probability of detecting an animal on the trackline (i.e., at a perpendicular distance of 0), or g(0), is affected by two factors: (1) availability bias, which is failing to detect animals because they are unavailable to be seen (e.g., hidden or submerged) and (2) perception bias, where observers fail to detect animals present at or near the surface (Pollock et al. 2006). Distance sampling assumes that g(0) = 1, but this is rarely the case in practice. This means g(0) is actually less than 1, and density and abundance will be underestimated because detectability will be assumed to be higher than it actually is unless correction factors are applied. Discussion of the g(0) adjustments applied to the density and abundance estimates follow.

3.4.3.1 Perception bias. No surveys obtained for this study had the requisite information to assess perception bias. None of the aerial surveys had a double observer protocol (aircraft lacked belly windows or two windows per side) which is required to assess perception bias *in situ*. The shipboard surveys did have two observer platforms (deck and A-frame) that could, in theory, be used for calculating perception bias; however, none of them had enough sightings on one platform to confidently assess perception bias. Sightings for shipboard surveys were low overall (see truncation distances in section 4.1), most likely due to sea turtles' low profile in the water.

Perception bias is generally low for animals that surface frequently or in large groups. Perception bias for large whales and small delphinids is generally close to one for shipboard surveys, though it is lower for aerial surveys given the higher speeds at which the aircrafts operate and the consequently shorter time available to sight animals (Palka et al. 2017 and Mannocci et al 2018b). Perception bias can be larger for animals that surface quickly or in small groups, like beaked whales and sea turtles. Because incorporating perception bias was not possible for this study, it is likely abundance/density is being underestimated. See section 5 for more detail on possible sources of over- and under-estimation of abundance.

3.4.3.2 Availability bias. From collaborators in the region, NUWC received three datasets of loggerhead sea turtles tagged with satellite-linked, time depth recorders that could be used for calculating dive and surface intervals appropriate for making g(0) adjustments (Oceanographic Turtles Project 2020, Hochscheid 2020, Chimienti et al. 2020, Hochscheid et al. 2013, Hochscheid et al. 2010, Hochscheid et al. 2007, Broderick et al. 2007, and the Society for the Protection of Turtles 2020). These tags recorded dive and surface intervals and were georeferenced, allowing for linking dives to specific locations. Because shipboard surveys are included in this study, it is important to calculate surface and dive intervals, rather than just the percent of time spent below the surface. Calculating surface and dive intervals is necessary because the relatively slow speed of survey ships results in longer time periods when areas are in view, allowing for a greater opportunity to sight animals when they come up for air. Aerial surveys, with their higher speed, can be treated as close to instantaneous, and a percent time below surface can be an appropriate adjustment.

Tagged animals from the three datasets were deployed in waters off Cyprus, Italy, and Spain. Animals ranged across all regions of the Mediterranean Sea included in this study except for the Adriatic Sea and Aegean Sea (figure 4). Because some of the data are unpublished, NUWC has agreed with the data providers not to show animal tracks and limit the reported results to the dive data summaries used to generate availability bias estimates. Table 3 summarizes the available data.

Table 3. Summary of Available Dive Data for Generated Availability Bias Estimates

Dataset	Number of tags	Number of dives	Years deployed	Life stages	Sex	Source	Primary regions
Cyprus	7	3,110	2002-2008	Adult	Female	Post-nesting	Alborán Sea/Strait of Gibraltar, Algero-Provençal Basin
Italy	31	11,985	2005-2017	Mix of adults, juveniles, and sub-adults (length, not age class, reported)	9 females, 4 males, 18 unknown	2 post-nesting, 16 rehabilitated, 13 wild-caught	Tyrrhenian Sea/eastern Ligurian Sea, Strait of Sicily/Tunisian Plateau/Gulf of Sirte, Ionian Sea/Central Mediterranean
Spain	17	36,279	2017-2020	1 adult, 15 juveniles, 1 unknown	2 female, 2 male, 13 unknown	14 wild-caught, 3 rehabilitated	Ionian Sea/Central Mediterranean, Levantine Sea

The Italy and Cyprus dive datasets had similar formats with dive duration and surface intervals given in seconds along with dates and times for the start and end of the dives. Georeferenced locations, a combination of global positioning system (GPS) and Argos satellite system locations, were provided separately along with dates and times. Argos locations of location classes 3, 2, 1, and 0 were considered valid locations as were all GPS locations. Dives were matched to the closest location within six hours. Dives that could not be georeferenced to a location within six hours were removed from the analysis.

For both of these datasets, tags were configured to consider a dive to have started when the turtle dove below 4 m (13 ft). In good viewing conditions (low turbidity, low Beaufort sea state, etc.) turtles can be seen as deep as 3 m (10 ft), though the chances of detecting turtles decreases as depth increases (Fuentes et al. 2014 and Barco et al. 2018). Because of this decreased detection chance, this likely overestimates the amount of time animals are available to be seen because some portion of the animals will be deeper than can be seen or will be harder to detect by observers. This would have the effect of underestimating density and abundance. NUWC did not try to quantify this additional source of perception bias, as was done in Fuentes et al. (2014) and Barco et al. (2018), because it is very condition specific.

Any surface intervals longer than four hours were removed. Surface times of this length could be indicative of a nesting event or a failure of the saltwater switch that indicated when the turtle was below the surface. Even though sea turtles are known to bask (Mrosovsky 1980), it was felt that this was a conservative measure given that underestimating availability bias was likely already occurring. These long surface intervals were less than one percent of all dive records.

Tags for the Spain dataset were formatted differently. Tags recorded depths over five-minute intervals and reported the average depth of the five-minute period. Each five-minute average depth was georeferenced to a location generated from a state-space switching model track of animal locations. These five-minute averages were then used to generate dive profiles. If there were gaps in the dive record, a new dive sequence was considered to have started. Surface and dive intervals were created from these dive profiles. Based on tag configuration, dives were defined to start when the turtles went below 3 m (10 ft), slightly shallower than the Italy and Cyprus datasets. Dives with surface intervals greater than four hours were eliminated to be consistent with the Italy and Cyprus datasets.

The way the Spain tags were formatted, short surfacing events of a few minutes or less may be missed. This is likely not an issue for aerial surveys, which can generally be treated as instantaneous snapshots of the surface, but this could be underestimating how long turtles are available at the surface for shipboard surveys (overestimating density and abundance). Despite not being formatted ideally for calculating availability bias, this dataset was included because the average dive and surface intervals were similar to the Cyprus and Italy datasets and it covered two regions of the Mediterranean Sea not covered by the other datasets (the Alboran Sea and the Algero-Provençal Basin).

The final combined dive dataset had 51,373 georeferenced dives. This dataset was then stratified spatially and temporally in three ways to determine if significant differences in dive behavior existed. First, turtles have diurnal changes in dive behavior (Hochscheid 2014), so NUWC identified daytime versus nighttime dives based on location, the time the dive was initiated, and local dawn/dusk times. Second, temperature changes substantially over the course of the year in the Mediterranean (Lazzari et al. 2012), that may change basking behavior for turtles. Neritic (coastal) turtle behavior in the Mediterranean also has been noted to increase in the summer as temperatures increase (Hochscheid et al. 2007). Therefore, dives were split into two seasons, winter and summer, based on major climatic shifts in temperature and observed increases in neritic turtle activity. Summer was defined as May through October and winter as November through April. Finally, differences in neritic versus deep water dives were assessed, where animals would presumably be feeding on different prey and exhibiting different dive behavior. Larger juvenile and adult loggerheads recruit to benthic foraging habitats where they feed primarily on benthic invertebrates while pelagic juveniles feed in the water column (Revelles et al 2007, Hochscheid et al. 2010, and Casale et al. 2018). This also partially addresses differences in behavior between larger, neritic adults and smaller, oceanic juveniles (Hochscheid 2014). Neritic areas were defined as regions shallower than 200 m (656 ft) (figure 6).

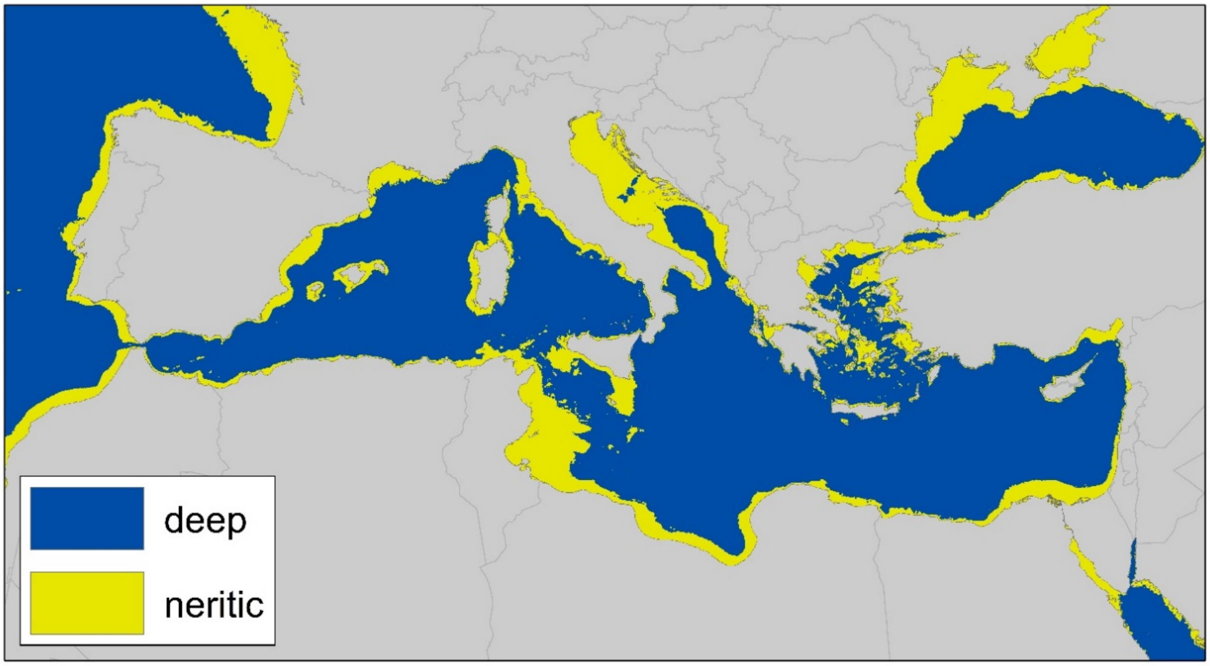

Figure 6. Regions within the Study Area Defined as Deep Water versus Neritic Habitat

Note: In figure 6, deep-water habitat is defined as waters greater than 200 m (656 ft) and neritic habitat is defined as waters less than 200 m (656 ft).

Significant differences in dive duration and surface interval were found by all three stratifications (t-test, p value < 0.05) (table 4). Based on this finding, to generate availability bias estimates, daylight dives only were used, which is when turtles would have been sighted in any case, and stratified by season and depth. This approach yielded four different availability bias adjustments based on the mean dive and surface intervals (table 5). There was high variability among the dives, and standard deviations of the intervals often exceeded the mean. This variability is not accounted for in the final model and bears more exploration in the future, including the possibility of creating a spatial model of availability. Instantaneous g(0) availability bias adjustments (surface interval/surface interval + dive duration) ranged from 0.48 for deep water areas in the summer to 0.27 in neritic areas in the winter (table 5).

Table 4. Surface and Dive Interval Means and t-Test p Values for Different Stratifications of Dive Data

Test	Mean 1 (s)	Mean 2 (s)	p value
Surface Interval by Diurnal Period	day - 1092	night - 1168	<0.001
Dive Duration by Diurnal Period	day - 1332	night - 1586	<0.001
Surface Interval by Depth	neritic - 549	deep - 1300	<0.001
Dive Duration by Depth	neritic - 1098	deep - 1535	<0.001
Surface Interval by Season	summer - 1105	winter - 1157	0.02
Dive Duration by Season	summer - 1151	winter - 2010	<0.001

Table 5. Stratified Availability Bias g(0) Estimates for the Mediterranean Sea

Season	Depth	Mean surface interval (s)	Mean dive duration (s)	Surface interval standard deviation (s)	Dive duration standard deviation (s)	No. of dives	g(0) instantaneous
summer	deep	1215	1306	2229	831	17102	0.48
winter	deep	1365	1781	2408	1412	5707	0.43
summer	neritic	551	716	2054	841	6549	0.43
winter	neritic	681	1868	1582	3413	1903	0.27

3.4.4 Per Segment Abundance Estimation

Abundance for each segment was calculated using a Horvitz-Thompson-like estimator:

$$\hat{N}_j = \sum_{r=1}^{R_j} s_{jr} / \hat{p}(z_{jr}) g(0)$$

,

where *Rj* was the number of observed groups in segment *j*, *sjr* was the size of the rth group in segment *j* , and *p̂*(*zjr*) was the estimated probability of detection given observation level covariates, *zjr*, and g(0) was the probability of detection on the trackline, here the availability bias estimate (Marques et al. 2007).

Availability bias was applied per segment, using mean surface and dive intervals specific to that location/season combination, and adjusted for the unique viewing properties and speed of the survey platform. For aerial surveys with bubble windows, the Caretta et al. (2000) formula was applied:

$$g(0)_{availability} = \frac{E[s] + t}{E[s] + E[d]}$$
,

where *E*[*s*] was the mean time spent at or near the surface, t was time when an animal was within visual range of the observer, and *E*[*d*] was the mean dive duration. This approach is appropriate when the observer has a clear view of the trackline, as is afforded by bubble windows, and the viewing area can be assumed to be square. Following Carretta et al. (2000), t = 10 seconds was used given the similarity in aircraft height and speed.

For aerial surveys that used flat windows, visibility was assumed to be impeded. Forcada et al. (2004) and Gomez de Segura et al. (2006) reported on this effect and the angles at which visibility became obstructed. Based on this, the Laake et al. (1997) equation (7) was applied using a mean effective strip width over the entire survey:

$$g(0)_{availability} = \frac{E[s]}{E[s] + E[d]} + \frac{w(x) - w(x)^2 0.5(\frac{1}{E[d]})}{E[s] + E[d]}$$
,

where *E*[*s*] was the mean time spent at or near the surface, *E*[*d*] was the mean dive duration, and the w(x) parameter was the amount of time the ocean was in the observer's view at a perpendicular distance x, given the vertical and lateral angles of obstruction. The w(x) parameter was calculated based on the aircraft properties reported in Gomez de Segura et al. (2006) for the Cessna 337 aircraft (the same aircraft used in the University of Valencia flat windows surveys).

For shipboard surveys, the Laake et al. (1997) equation (4) was applied to derive g(0) for each survey following Cañadas and Vázquez (2014):

$$g(0)_{availability} = \frac{E[s]}{E[s] + E[d]} + E[d]\left(\frac{1 - \exp\left(-\frac{1}{E[d]} r/s\right)}{E[s] + E[d]}\right)$$
,

where *E*[*s*] was the mean time spent at or near the surface, *E*[*d*] was the mean dive duration, *r* was the maximum forward distance at which animals could reasonably be expected to be detected (assumed to be the 90th percentile of radial distances, as in Cañadas and Vázquez 2014), and *s* was the mean vessel speed. *r* and mean speed were calculated for each aerial survey.

3.5 SPATIAL MODELING

3.5.1 Environmental Covariates

Covariates that could be associated with marine turtle habitat derived from ocean models and remotely sensed data were included as possible explanatory covariates for the model. Six static covariates and ten dynamic covariates (three physical and seven biological) that were available at a monthly resolution, were analyzed as candidate covariates for the density models (table 6). Only contemporaneous environmental dynamic covariates were included in the models, rather than climatological covariates, on the assumption that turtle distribution is more closely related to ephemeral conditions than long-term averages of conditions (Howell et al. 2015).

In addition to the below listed covariates, a seabed habitat map was explored as a candidate covariate (Populus et al. 2017) but was ultimately not included in the analysis after initial model fitting and prediction. While its inclusion offered minor improvements to deviance explained and slightly lower relative maximum likelihood (REML) scores than other models, it greatly increased uncertainty. NUWC staff did not feel this was a worthwhile tradeoff, and it was eliminated from consideration.

All covariates were processed to a 5 x 5 km (3 x 3 mi) grid using a nearest neighbor resampling method and projected into a regional coordinate system using ArcGIS (version 10.7), the Marine Geospatial Ecology Tools software (Roberts et al. 2010), and custom Python and command prompt scripts. No interpolation or extrapolation was required as all covariates covered the entire Study Area.

A spatial smooth was not included as a covariate in the model. Including spatial smooths is a common practice in density spatial modeling to account for variability not captured by the available environmental covariates. It was not used here because a spatial smooth cannot be extrapolated, which would necessitate using separate models for any areas of geographic extrapolation, and because a spatial smooth requires even survey coverage.

Table 6. Candidate Environmental Covariates for Inclusion in Density Spatial Models

Candidate environmental covariates	Source
Biological	
Chlorophyll	Monthly mean chlorophyll concentration at the ocean surface derived from the Mediterranean Sea Biogeochemical Reanalysis ocean model (Teruzzi et al 2019)
Net Primary Productivity	Monthly mean primary production at the ocean surface derived from the Mediterranean Sea Biogeochemical Reanalysis ocean model (Teruzzi et al 2019)
Phytoplankton Carbon Biomass	Monthly mean phytoplankton carbon biomass at the ocean surface derived from the Mediterranean Sea Biogeochemical Reanalysis ocean model (Teruzzi et al 2019)
Vertically Integrated Chlorophyll	Monthly mean of depthwise integration of chlorophyll concentration through the photic zone (Teruzzi et al 2019)
Vertically Integrated Net Integrated Primary Productivity	Monthly mean of depthwise integration of net primary productivity across the water column (or photic zone) (Teruzzi et al 2019)

Table 7. Candidate Environmental Covariates for Inclusion in Density Spatial Models (Cont'd)

Candidate environmental covariates	Source
Biological	
Vertically Integrated Phytoplankton Carbon Biomass	Monthly mean of depthwise integration of phytoplankton carbon biomass across the water column (or photic zone) (Teruzzi et al 2019)
Vertically Generalized Production Model (VGPM)	Monthly net primary productivity across the water column by the VGPM model (Behrenfeld & Falkowski 1997)
Physical	
Sea Surface Temperature	Monthly mean sea surface temperature at the ocean surface derived from the Mediterranean Forecasting System ocean models (Nucleus for European Modeling of the Ocean (NEMO) (Simonceli et al. 2019)
Bottom Temperature	Monthly mean temperature at the ocean bottom derived from the Mediterranean Forecasting System ocean models (NEMO) (Simonceli et al. 2019)
Salinity	Monthly mean salinity at the ocean surface derived from the Mediterranean Forecasting System ocean models (NEMO) (Simonceli et al. 2019)
Static	
Depth	Depth of seafloor derived from Shuttle Radar Topography Mission (SRTM)15 and SRTM30 bathymetry (Becker et al. 2009 and Olson et al. 2016)
Slope	Slope of seafloor derived from SRTM15 and SRTM30 bathymetry (Becker et al. 2009 and Olson et al. 2016)
Distance to Canyon	Distance to closest submarine canyon derived from the International Hydrographic Organization-International Oceanographic Commission's General Bathymetric Chart of the Oceans Gazetteer (IHO-IOC Commission 2018).
Distance to Seamount	Distance to closest seamount derived from Wurtz and Rovere (2015)
Distance to Shore	Distance to shore derived from National Oceanic and Atmospheric Administration (NOAA 2016)
Seabed Habitat Map	Seabed habitat derived from Europe SeaMap (Populus et al. 2017)

3.5.2 Extrapolation Assessment

There are three types of extrapolation to consider for spatial density models: (1) geographic extrapolation, where predictions are made in unsurveyed areas, (2) temporal extrapolation, where predictions are made in unsurveyed time periods, and (3) environmental extrapolation, where predictions are made into novel environmental conditions. Areas that are not extrapolated are interpolations. Knowing where and when one is extrapolating is important as one has more confidence in the results of interpolations.

Previous work by the Duke team assessed the extent of environmental extrapolation in the Mediterranean Sea based on surveys from 2003 through 2016 (Mannocci et al. 2018a). In this study, the ASI surveys were added, necessitating a reassessment of the extent of extrapolation for the study.

Environmental extrapolation can be either univariate or combinatorial (i.e., multivariate). Univariate extrapolation occurs when the researcher predicts outside the environmental envelope of a single covariate. Imagine the researcher has sampled temperature ranging from 25 to 30° C (77 to 86° F) but made a prediction in an area of 32° C (90° F). This would be univariate extrapolation. Combinatorial extrapolation occurs when the researcher predicts two novel combinations of covariates.

Environmental extrapolation was evaluated using the R package dsmextra (Bouchet et al. 2019). Specifically, the dsmextra implementation of the ExDet (Mesgaran et al. 2014) tool to assess the extent of univariate and combinatorial extrapolation. Gower's distance calculations were not implemented to assess how near extrapolated locations were to interpolated locations. When running the Gower's distance tool in dsmextra on a single month of their dataset, it took an unreasonably long time to process, making calculations for all 192 months of the study period infeasible.

Extrapolation was assessed both seasonally and annually. Seasons were defined as May through October for summer and November through April for winter. See section 3.5.3 for a more detailed discussion on how seasons were defined. About 77 percent of the survey effort was expended during summer months and 23 percent during winter months.

For annual models, geographic extrapolation occurred over 16 percent of the Study Area and was largely limited to territorial seas and Exclusive Economic Zones (EEZs) in the Southern Mediterranean (figure 7(a)). The political climate in many countries that border the Southern Mediterranean Sea precludes safely entering those areas with survey platforms.

In summer, geographic extrapolation was also 16 percent, which was unsurprising given that most surveys occurred in summer months. In winter, geographic extrapolation was 79 percent of the Study Area. Available winter survey data were limited to the central and North-central Mediterranean and some limited areas in the Western Mediterranean. Survey coverage was completely absent from the Eastern Mediterranean, Adriatic Sea, and Aegean Sea in the winter (figure 7(b)).

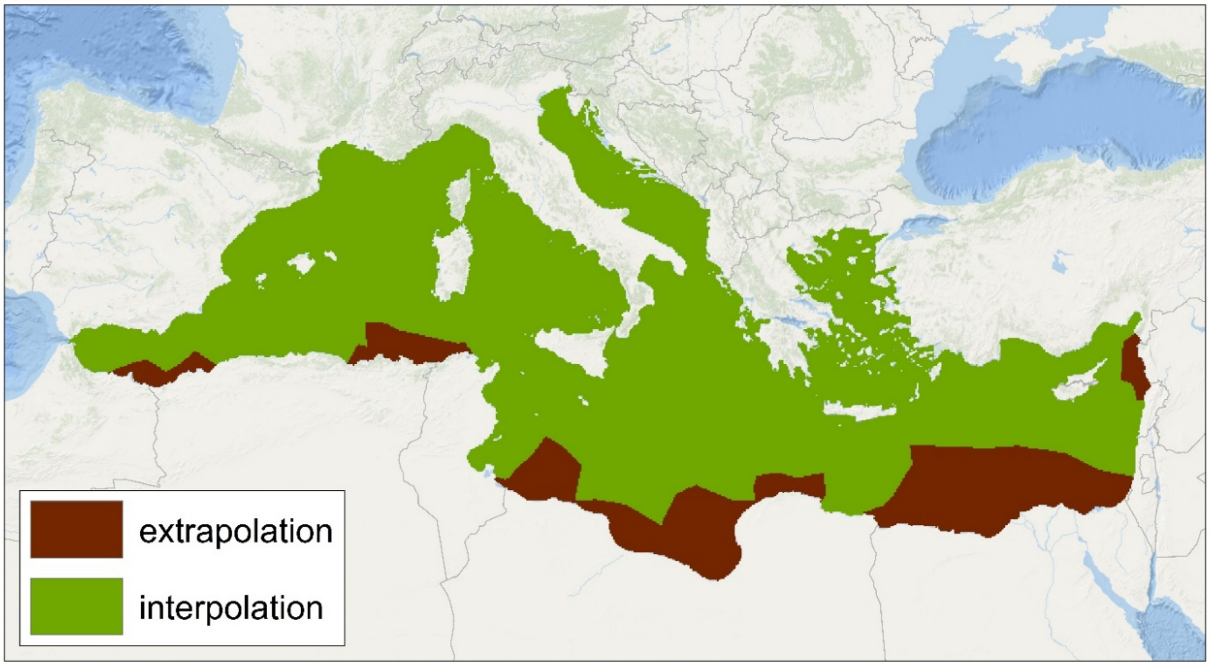

a

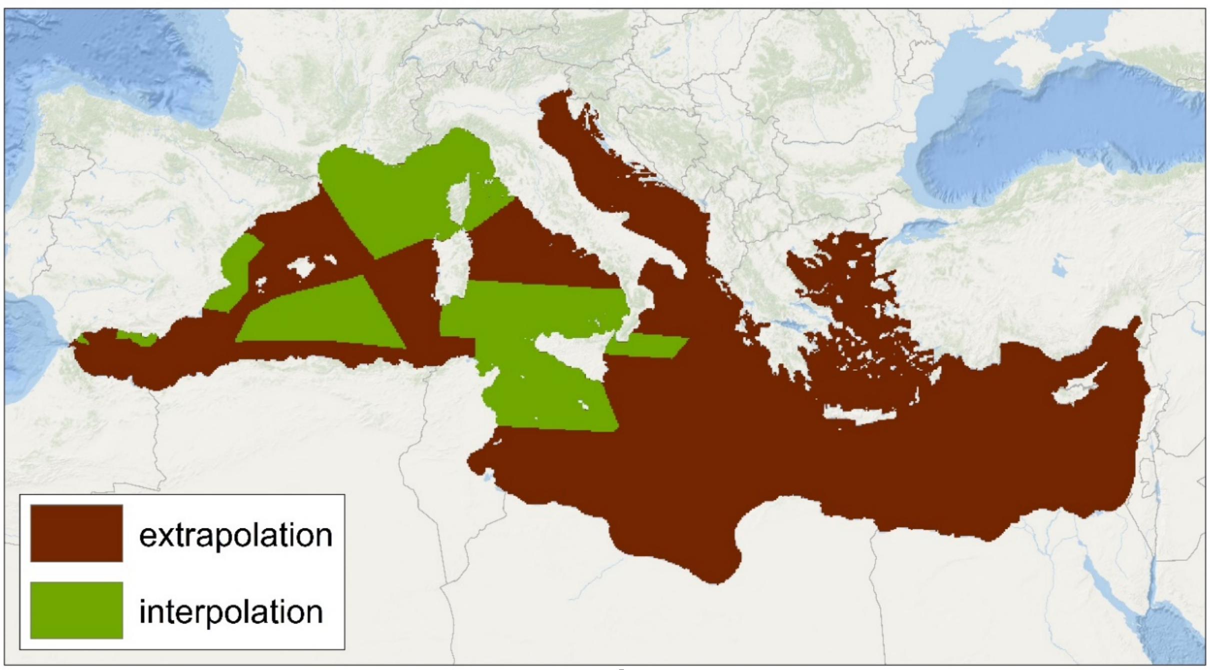

b

Figure 7. Extent of Geographic Extrapolation

Note: In figure 7, the extent of extrapolation is shown for Annual Models in the Summer Models (a) and Winter Models (b).

The temporal resolution of density predictions for this project is monthly; therefore, the finest scale at which temporal interpolation was assessed was monthly. Out of the 192 months covered by the study, 135 months (70 percent) did not have any survey coverage anywhere in the Mediterranean. Aggregating by year, there were three years without any survey coverage, seven years if the aggregate is by year and season combined (table 7). When aggregating by month, all months of the year contained survey data.

Table 8. Temporal Interpolation and Extrapolation Summary

Year	Annual	Summer	Winter
2003	219	219	0
2004	231	139	92
2005	0	0	0
2006	1141	975	166
2007	1857	1489	368
2008	686	563	123
2009	3950	2316	1634
2010	6257	6033	224
2011	2245	228	2017
2012	5194	3655	1539
2013	4053	3584	469
2014	1338	0	1338
2015	0	0	0
2016	1415	0	1415
2017	0	0	0
2018	11494	11494	0
Years without data	**3**	**5**	**5**
Years without data (extrapolations) are highlighted. Values are linear km of survey effort.			

Environmental extrapolation when using all survey data was low (annual models). On average, less than two percent of areas had univariate extrapolation in any month. The maximum was six percent, and there was no combinatorial extrapolation, which is reasonable given the low amount of univariate extrapolation. To visualize extrapolation over the entire study period, monthly rasters were reclassified into areas with and without extrapolation, one and zero, respectively. All the rasters were then summed for the entire study period. The result was a single raster showing the number of months in the study period where there was extrapolation (figure 8). The area of high extrapolation North of Libya was driven by the distance to canyon covariate, and the area in the North Adriatic Sea was driven by low salinity values. Areas with outflows near other major rivers showed similar patterns.

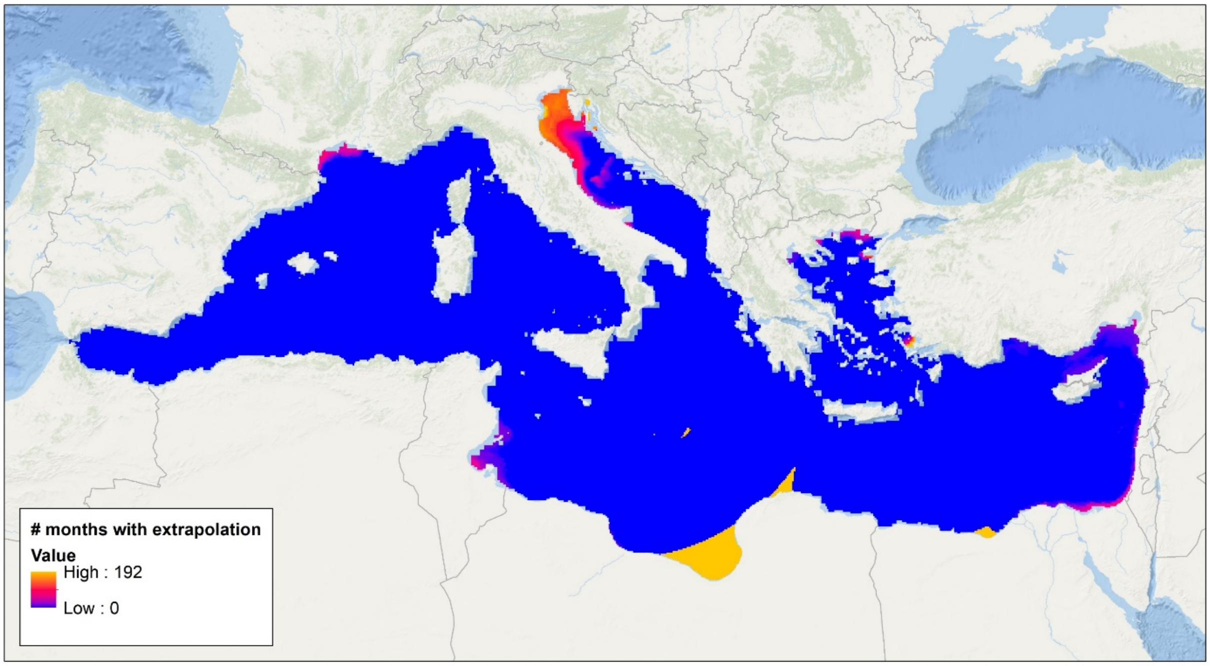

Figure 8. Months with Environmental Extrapolation for Annual Models

For summer months (77 percent of survey data), mean univariate extrapolation was 18 percent per month, with a maximum of 72 percent. There was no combinatorial extrapolation. Extrapolation was driven by distance to canyon and sea surface temperature and was generally highest in the Western Mediterranean Sea (figure 9). Eliminating distance to canyon and sea surface temperature as candidate covariates dropped the mean extrapolation per month to less than one percent, with salinity contributing the most to extrapolation. Extrapolation remained high in the Northern Adriatic Sea but was low elsewhere except for a few coastal areas (figure 9).

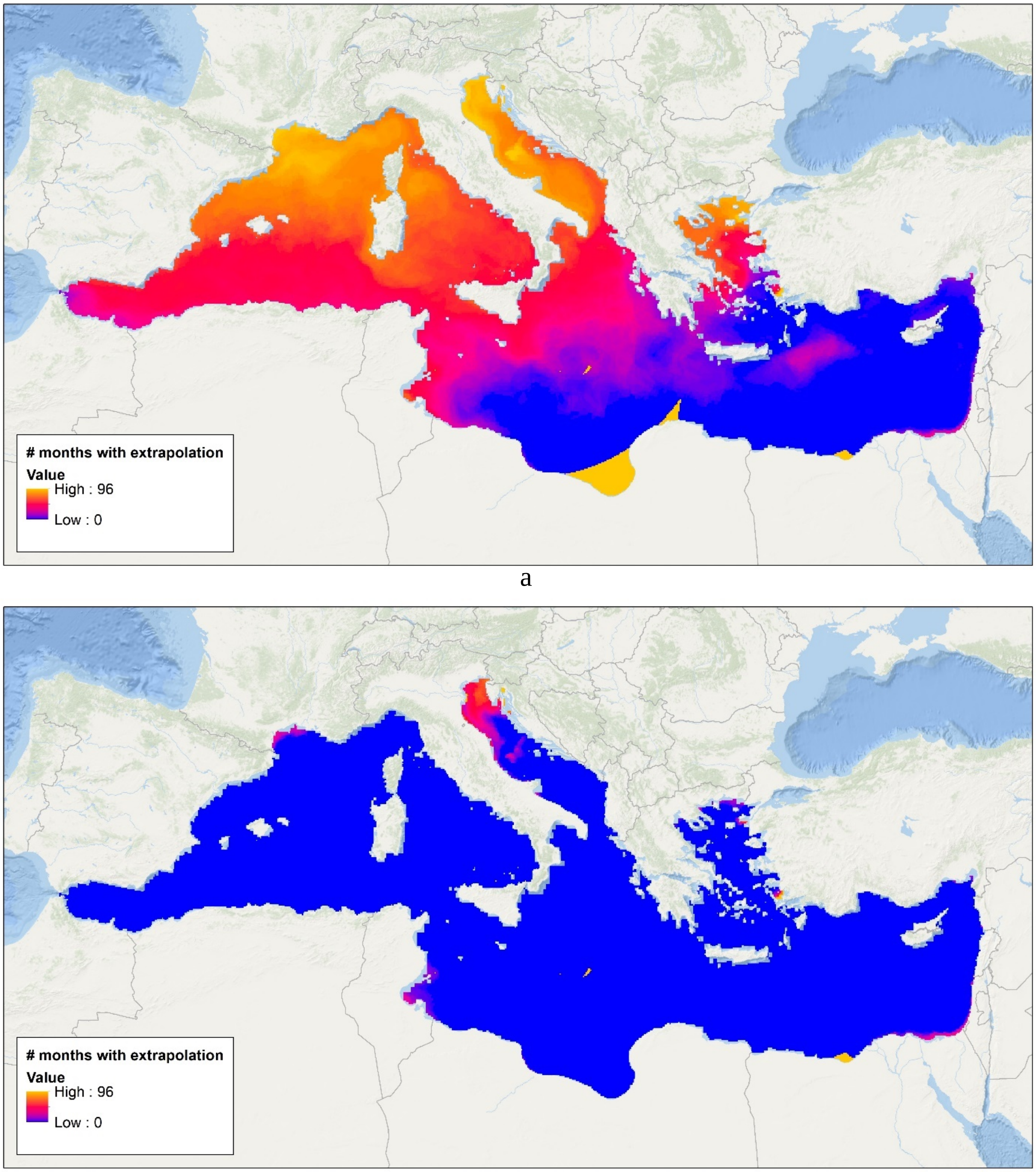

Figure 9. Number of Months with Extrapolation during Summer

Note: In figure 9, the number of months is shown for all candidate covariates (a) and all candidate covariates except distance to canyon and sea surface temperature (b).

For winter months (23 percent of survey data), mean univariate extrapolation was 75 percent per month and there were 28 months with 100 percent extrapolation, meaning at least one covariate in each grid cell was unsampled by the available survey data. There was a small percentage of cells in each month with combinatorial extrapolation. Extrapolation was driven by distance to canyon, distance to seamount, and sea surface temperature. Extrapolation was 100 percent in the Eastern Mediterranean Sea in all months. No surveys occurred in the Eastern Mediterranean in the winter (figure 10).

Eliminating distance to canyon, distance to seamount, and sea surface temperature as candidate covariates improved the situation to some extent; however, mean univariate extrapolation remained high at 49 percent, with salinity then contributing the most to extrapolation. Extrapolation remained at 100 percent in some areas of the Eastern Mediterranean and in the Northern Adriatic Sea (figure 10). This high level of extrapolation in winter made fitting winter models challenging and caused low confidence in results for that season.

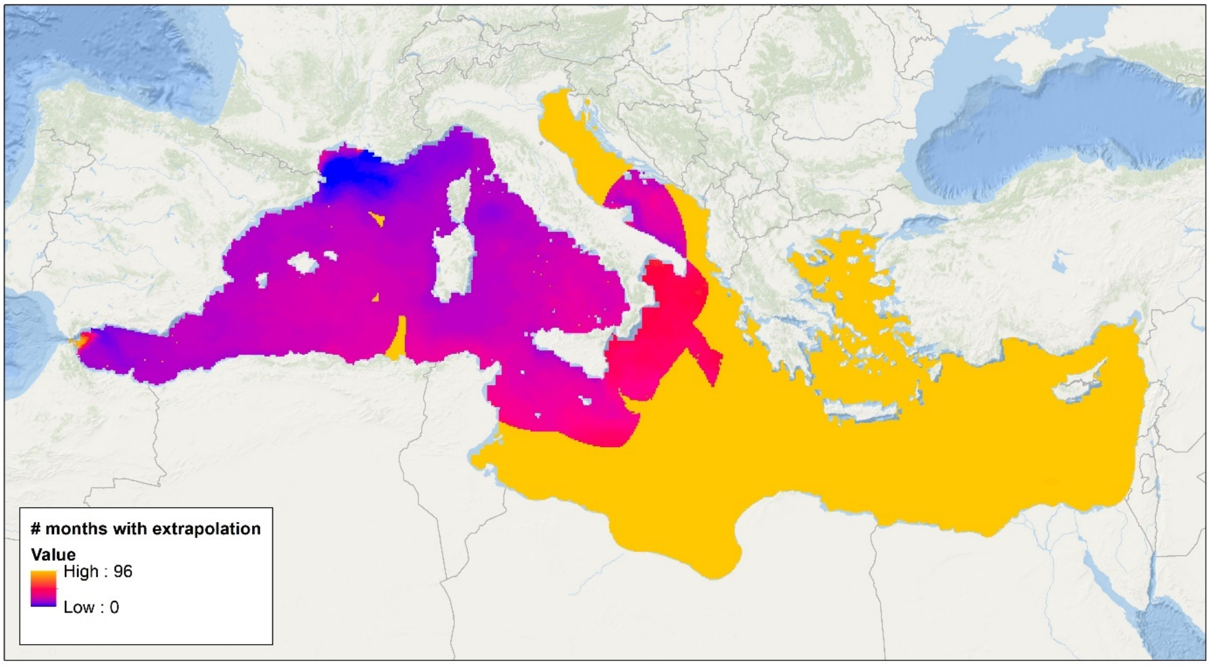

a

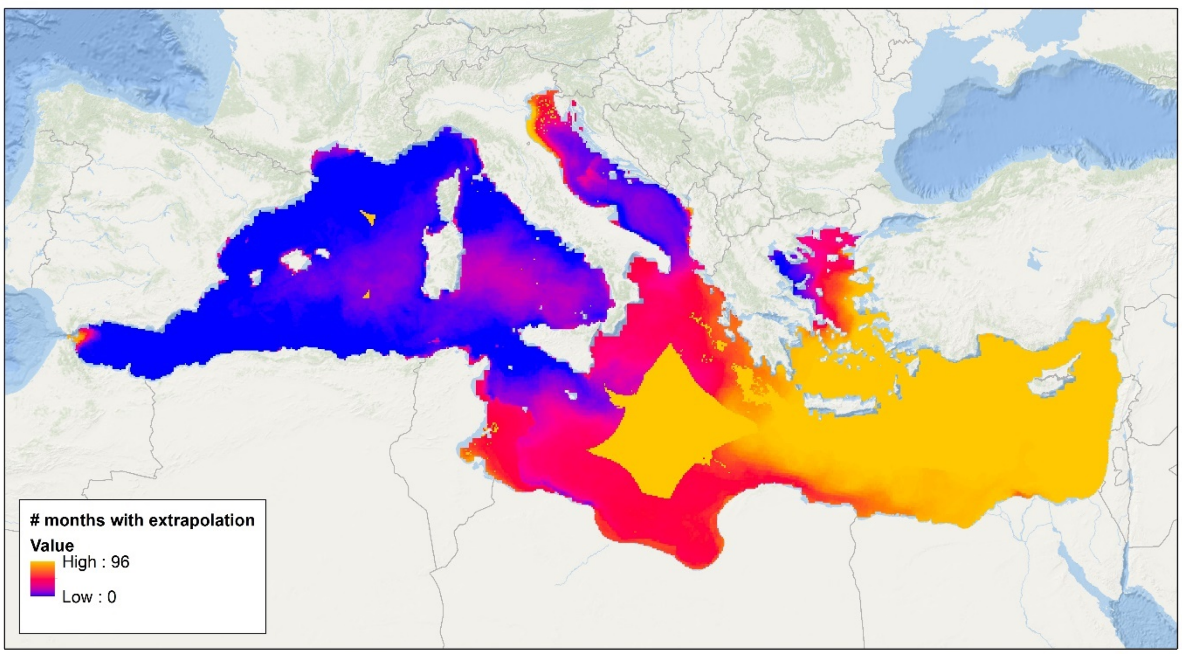

b

Figure 10. Number of Months with Extrapolation during Winter

Note: In figure 10, the number of months is shown for all candidate covariates (a) and all candidate covariates except distance to canyon, distance to seamount, and sea surface temperature (b).

3.5.3 Density Modeling

A generalized additive model (GAM) framework as used for all models with the following general form:

$$\mathbb{E}(\hat{N}_j) = A_j \exp\left[\beta_0 + \sum_k f_k\left(z_{jk}\right)\right],$$

Nj was the estimated abundance in segment j. The response variable was assumed to follow a Tweedie distribution (Foster & Bravington 2013), which handles zero-inflated distributions well. This is useful because most segments had zero sightings and, therefore, an abundance of zero. E indicates expectation; *Aj* was the model offset, the area of segment *j* calculated as 2(wR-wL)lj, where wR was the right-truncation distance, wL was the left-truncation distance (0 if data were not left truncated), and lj was the segment length; *fk* were smooth functions of the sampled environmental covariates zjk; and β0 was the model intercept. All models were fit with the R package mgcv (version 1.8-31; Wood 2011).

Models were fit to all segments from survey data between 2003 and 2018. Two different modeling approaches were attempted. First, modeling was done with unlimited numbers of the available covariates and allowing maximum degrees of freedom, or wiggliness, for their relationship to the response variable. Thin-plate regression splines with shrinkage were used to allow the effect of non-significant variables to shrink away to zero (Wood 2003). Second, more parsimonious models were run, limited to four covariates and four degrees of freedom that capture dominant abundance-environmental relationships but not fine-scale detail in the data (Elith et al. 2010). The second type of model is useful for situations where extrapolation occurs.

In both modeling approaches, many models were fit, with all possible combinations of available covariates attempted. The exception was covariates that were highly correlated. Correlation was examined using Spearman's correlation coefficient, and if covariates had a score of 0.5 or higher, only one was retained. Selection between correlated covariates occurred by fitting single covariate models to the data and performing model selection. Model selection was accomplished by choosing the model with the lowest REML score for both the single and multi-covariate models. REML was selected as the criterion for estimating smooth parameters and discriminating between models because it penalizes overfitting and leads to more pronounced optima (Wood 2011).

All the productivity covariates were correlated with each other. Chlorophyll a had the best performance. The different versions of bathymetry and slope covariates were also correlated. Between the bathymetry options, SRTM15 was selected, and SRTM30 derived slope was selected from the slope covariates.

Models were checked by examining Q-Q plots, residuals, utilized degrees of freedom, and by qualitatively assessing models for unrealistic artifacts or predictions. A qualitative assessment of the relative merits of the unlimited versus parsimonious predictions was also made. Covariates in the parsimonious suite of models were limited to those that minimized extrapolation.

Predictions were made on a monthly basis, as that was the finest temporal scale of the selected covariates. Between 2003 and 2018, there were 192 monthly predictions. Both annual and seasonal models were fit, as there is evidence that animals migrate seasonally from the Eastern to Western basins and from the Eastern basin to the Adriatic (summarized in Casale et al. 2018). Seasons were defined as summer, May through October, and winter, November through April. This definition was based on the predominant warming and cooling cycles in the Mediterranean Sea, which also track wind driven productivity cycles (Lazzari et al. 2012), and when larger neritic turtles become more active as temperatures warm (Broderick et al. 2007 and Hochscheid et al. 2007). A four-season model was not attempted as there was no evidence that turtles have four distinct behavioral states segregated by seasons in the Mediterranean Sea.

Annual models were averaged into a single prediction covering the time span of the study period, creating a densitology prediction of long-term density and abundance over the 16 years. Seasonal models were aggregated by averaging all the months in the seasonal definition over the 16-year study period. Inter- and intra-annual variability were assessed by examining plots of monthly predicted abundance over time.

3.5.4 Uncertainty Estimation

Because there are many components that contribute to the density and abundance prediction, there are many sources of uncertainty and variability in the model. There is no simple way to account for and combine all sources of uncertainty in the model, but it is important to acknowledge their existence and estimate uncertainty, where feasible. Sources of uncertainty and variability include; uncertainty in the detection functions, measurement error in distances to sightings, variability in dive behavior, environmental variability, uncertainty in covariate measurements, and uncertainty in model parameter estimation.

For this project, two sources of uncertainty were accounted for explicitly: model parameter uncertainty and environmental variability, expanding on Becker et al. (2014). After model fitting and selection, parameter estimates from the selected model were resampled based on their associated uncertainty and new predictions were made from the resampled parameters. The process was repeated 200 times for each month, creating a set of 200 predictions for each month that varied based on the uncertainty of the parameter space of the selected model relative to the underlying environment. The coefficient of variation (CV) was calculated based on these predictions, which combined the model parameter uncertainty and environmental variability. These CVs were averaged into both a single value and a surface (similar to the densitologies) so that how uncertainty varied spatially could be examined.

Work is underway by the Navy-funded DenMod working group to incorporate more types of uncertainty into density models like the ones here (e.g., multiple surveys, detection functions, long-term averages of density). Currently, the only available methods are prohibitive from a time and computation perspective. In the interim, it must berecognized that uncertainty and variability in the predictions are being underestimated and that any reported CV only accounts for a portion of the variability in the model. In particular, the data used for availability bias were highly variable (table 5).

4. RESULTS

4.1 DETECTION FUNCTIONS

Table 8 summarizes the selected detection function, covariates, and truncation distances for all surveys, Further details and considerations for each survey are also provided.

Table 9. Summary of Selected Detection Functions

Survey*	Platform	Selected function	Covariates	Truncation distance
ASI	Aerial	N/A	N/A	N/A
BWI ISPRA	Aerial	Hazard rate	Glare, Beaufort sea state, month	Right truncation at 343 m
PELAGIS	Aerial	Half-normal	Beaufort sea state, month	Right truncation at 200 m
TETHYS ISPRA	Aerial	Half-normal with cosine adjustment	None	Right truncation at 300 m
University of Valencia	Aerial	Half-normal	Month	Right truncation at 450 m, left truncation at 104 m
Alnitak/Alnilam	Shipboard	Hazard rate	Month, observer position	Right truncation at 400 m
Song of the Whale (IFAW/MCR)	Shipboard	Hazard rate	Beaufort sea state	Right truncation at 100 m
Song of the Whale (ASI)	Shipboard	Hazard rate	Month	Right truncation at 100 m

*Full names of survey providers were provided in table 1.

ASI aerial survey: As mentioned previously, the ASI aerial survey recorded sea turtle and seabird sightings using a strip transect methodology. Therefore, no detection function was fit for these data.

BWI ISPRA aerial survey: 25 sightings were removed that were missing perpendicular distances and one sighting that was missing detection covariates. Associated segments were removed from the analysis. Initally, separate detection functions were fit to each year of the survey as there were enough sightings in each year to support this. However, the histograms of sightings versus perpendicular distance showed some heaping and potential guarding of the trackline. The Q-Q plots for individual years bore this out.

The histogram for all years combined improved the heaping issue near the trackline, resulting in a histogram where sighting probability decreased away from the trackline as expected, especially once the data were right truncated (figure 11) at 343 m (1,125 ft) to maintain a 15 percent probability of detection threshold. The selected detection function was the hazard rate with glare, Beaufort sea state, and month as covariates. Year was included as a possible covariate in the combined detection function to account for effects between surveys, but it was not selected.

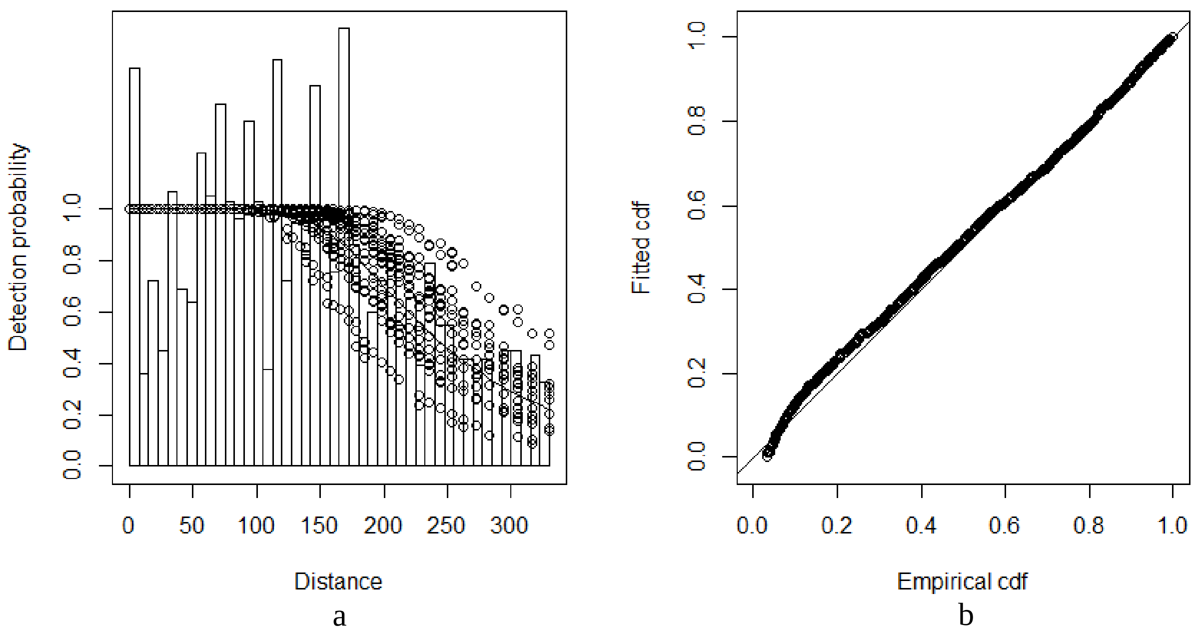

Figure 11. Detection Function for the BWI ISPRA Aerial Survey

Note: In figure 11, the fitted hazard rate detection function with glare, Beaufort sea state, and month as covariates (a) and associated Q-Q plot (b).

PELAGIS aerial survey: All on effort sightings had data for all environmental covariates and perpendicular distances. The data were right-truncated at 200 m (656 ft) to maintain a 15 percent probability of detection threshold. The selected detection function was the half-normal with month and Beaufort sea state as covariates.

There were only two sightings in Beaufort sea state 4, so when Beaufort sea state was selected as a covariate, it was decided to eliminate these segments (83 segments out of 6,442) as there were too few sightings in these conditions to create a functional relationship for that category. Figure 12 shows the selected detection function and Q-Q plot.

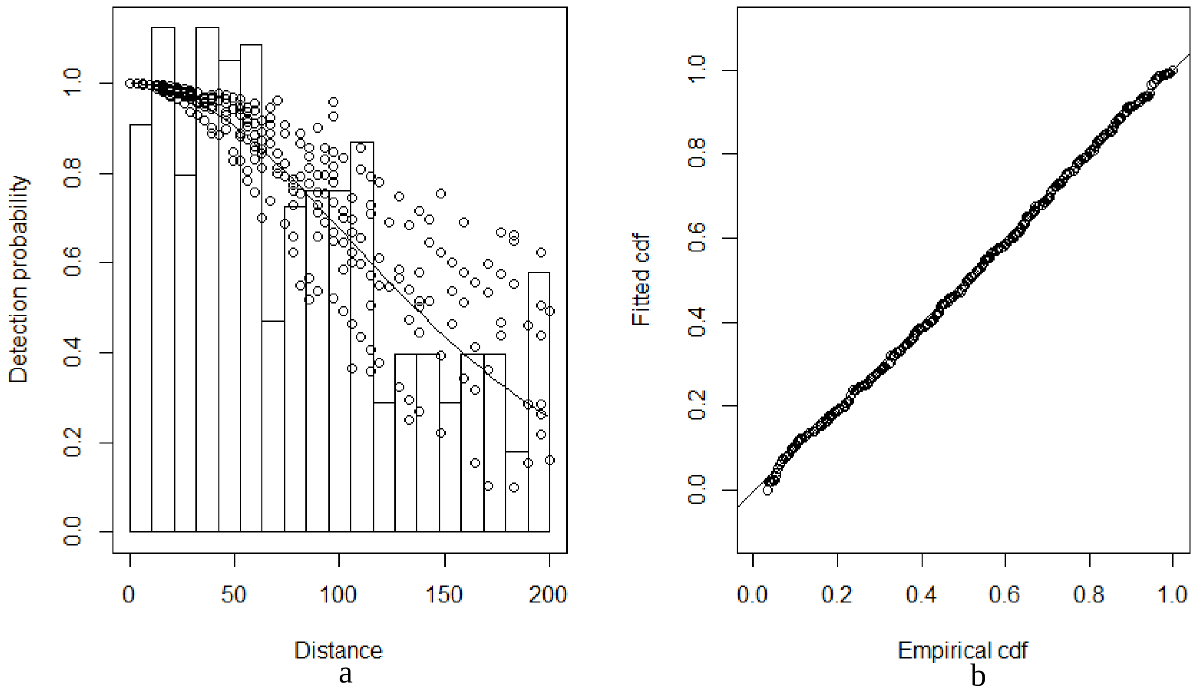

Figure 12. Detection Function for the PELAGIS Aerial Survey

Note: In figure 12, the fitted half-normal detection function with month and Beaufort sea state as covariates (a) and associated Q-Q plot (b).

TETHYS ISPRA aerial survey: 16 sightings were missing perpendicular distances, and those sightings, as well as their segments, were eliminated. The maximum sightings distance was 2.5 km (1.5 mi). The data were right-truncated at 300 m (984 ft) to maintain a 15 percent probability of detection threshold. Of the available covariates, only turbidity was not included in the analysis as there were only 10 non-zero values, not enough to fit a relationship.

A half-normal model with a cosine adjustment performed better than all attempted models that included covariates. There was some potential heaping/guarding on the trackline (see the spike at distance zero in figure 13) and there was no clear way to address this heaping. However, detection functions are generally robust to this kind of heaping, and the normal model selection process was used.

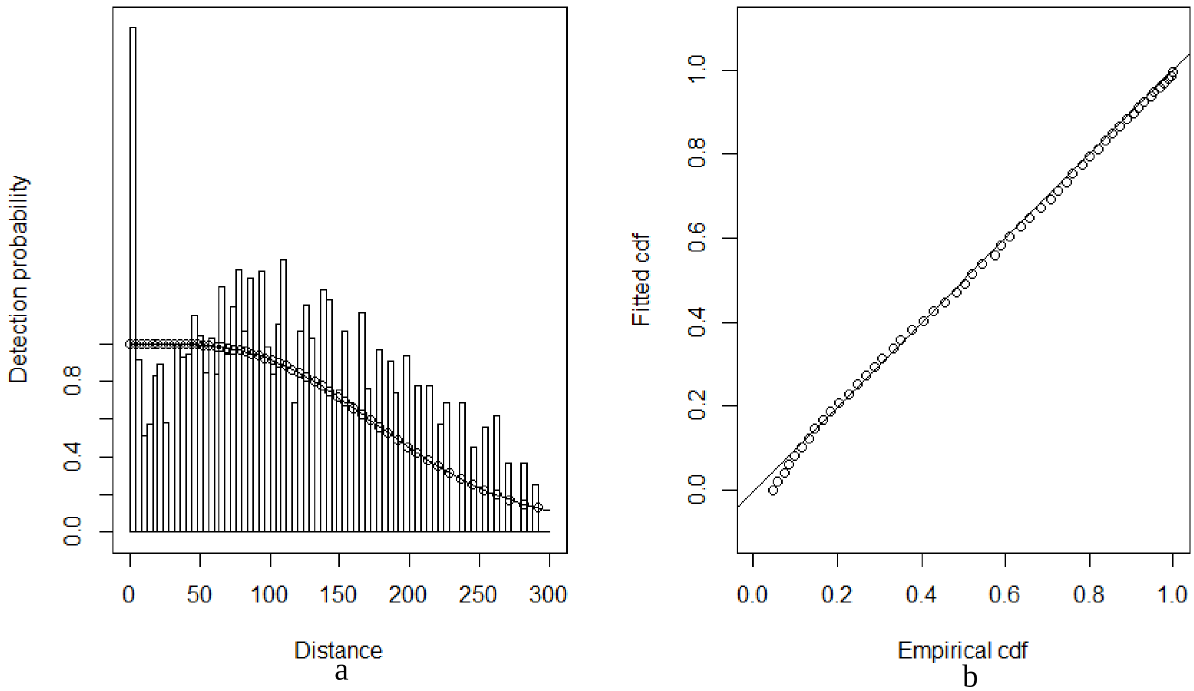

Figure 13. Detection Function for the TETHYS ISPRA Aerial Survey

Note: In figure 13, the fitted half-normal detection function with cosine adjustment (a) and associated Q-Q plot (b).

University of Valencia aerial survey: Four sightings without perpendicular distances and their associated segments were removed. Surveys were flown at different heights in 2010/2011 and 2013, so initially an attempt was made to fit separate models to these surveys. There were only 34 sightings in the 2010/2011 surveys. The Q-Q plots for models fitted to those surveys indicated poor fit and were unable to include any covariates, so the decision was made to combine them and include the survey as a potential covariate.

The selected detection function was the half-normal, left truncated at 104 m (341 ft) and right truncated at 450 m (1,476 ft), with month as the only covariate. See section 3.4.2 for an explanation of the need for left truncation. The Q-Q plot (figure 14) was not as good as in other aerial surveys, but this was unsurprising given the relatively lower number of sightings, the need for left truncation, and the different altitude between years.

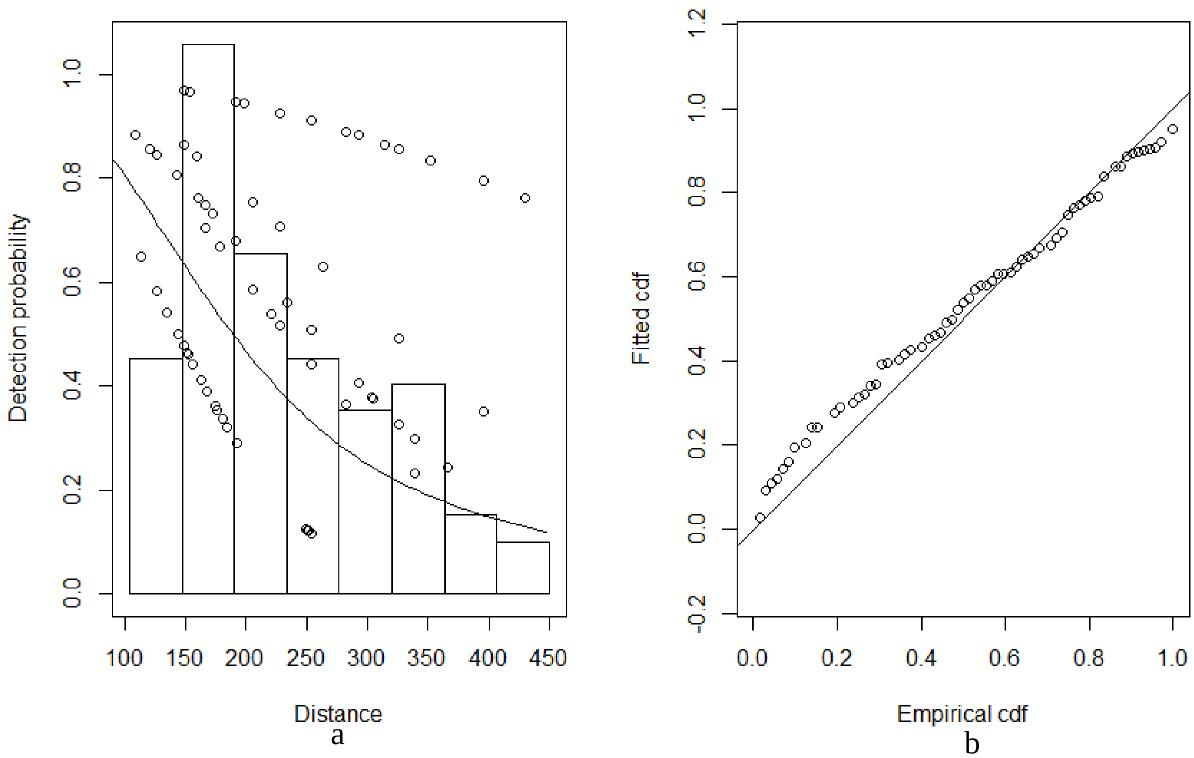

Figure 14. Detection Function for the University of Valencia Aerial Surveys

Note: In figure 14, the fitted half-normal detection function with month as a covariate (a) and associated Q-Q plot (b).

Alnitak/Alnilam shipboard surveys: One sighting and associated segment was deleted that did not have a location for the sighting. Though Beaufort sea state was collected, a decision was made not to include it as a potential covariate as there were many missing values associated with the sightings.

All data pre-2006 where perpendicular sightings were not recorded for turtles were removed from the analysis. Section 3.4.2 details why these decisions were made. The selected detection function was the hazard rate with month and observer position as covariates and right truncated to 400 m (1,312 ft) to meet the 15 percent probability of detection threshold. Observer position was included as the deck and A-frame observer positions were at different heights, which could affect detectability. These two sets of sightings were combined as there were not enough A-frame sightings to fit a separate detection function (figure 15).

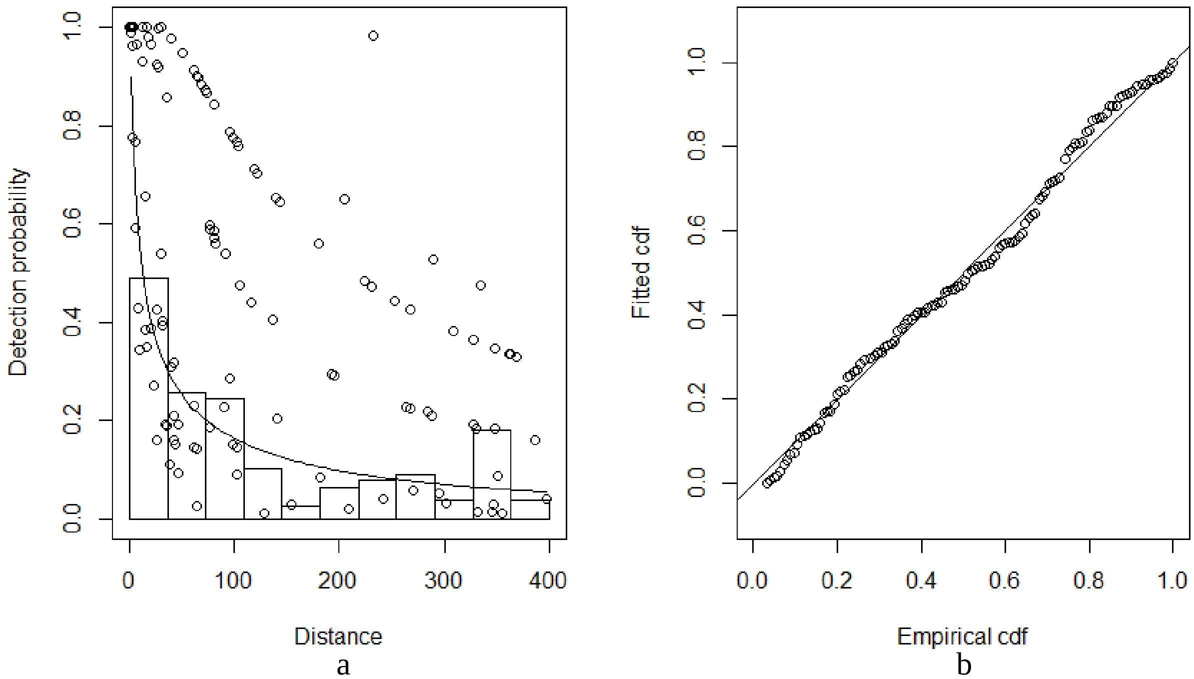

Figure 15. Detection Function for the Alnitak/Alnilam Shipboard Surveys

Note: In figure 15, the fitted hazard rate detection function with month and observer position as covariates (a) and associated Q-Q plot (b).

Song of the Whale (IFAW/MCR) shipboard survey: Three sightings without perpendicular distances, along with associated segments, were removed. There was missing data for the cloud cover, observer, cue, and behavior covariates, so these were not included as possible covariates.

Sightings dropped off sharply with distance, necessitating right truncation at 100 m (328 ft). Even this sharp truncation yielded only a 10 percent probability of detection threshold. A decision was made not to truncate further as only 43 sightings were left after truncating at 100 m (328 ft). Because of this limitation, for this survey no more than one covariate was included in the detection function. The hazard rate function was selected with Beaufort sea state as a covariate (figure 16).

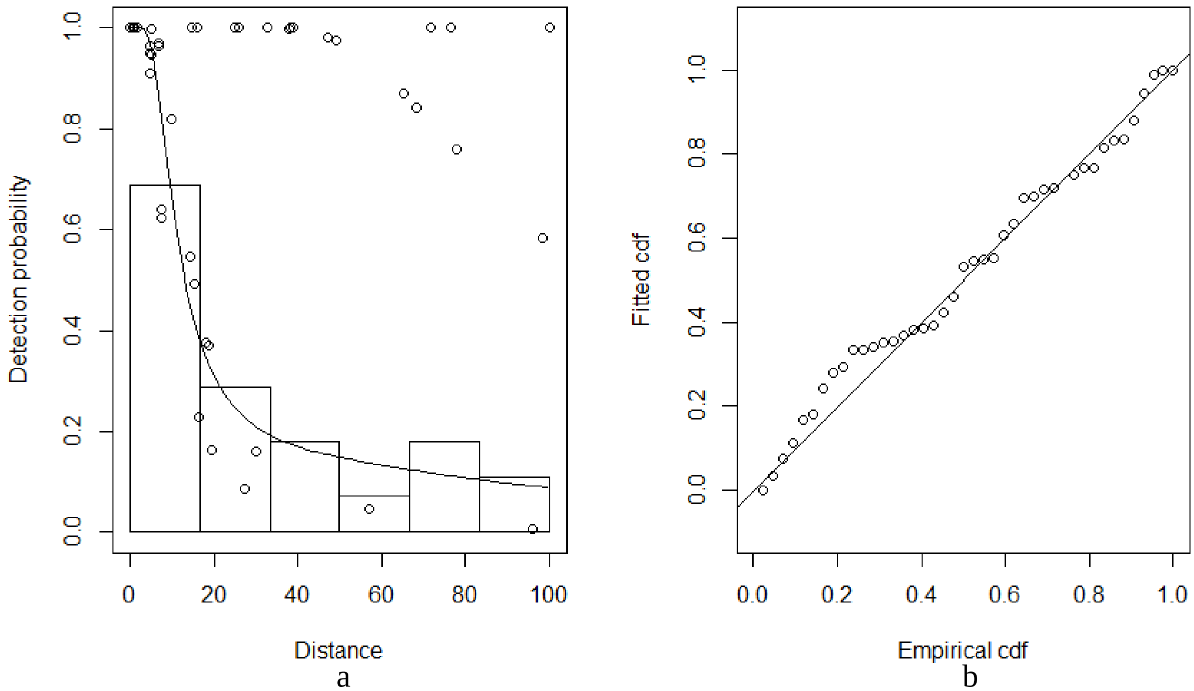

Figure 16. Detection Function for the Song of the Whale (IFAW/MCR) Shipboard Surveys

Note: In figure 16, the fitted hazard rate detection function with Beaufort sea state as a covariate (a) and associated Q-Q plot (b).

Song of the Whale (ASI) shipboard survey: Even though the ASI shipboard survey was performed by the same group as the IFAW/MCR shipboard survey, a separate detection function was fit because the ASI shipboard survey was paired with the ASI aerial survey and represented one of the most recent surveys in the Mediterranean Sea.

Similar to the other Song of the Whale survey, the data needed to be right-trucated at 100 m (328 ft) to maintain a 15 percent probability of detection threshold. This retained more than 80 sightings, so the normal model fitting and selection process was used. There were A-frame versus deck sightings, and though there were not enough deck sightings to fit a separate detection function, observer position was included as a potential covariate. The detection function selected was hazard rate with month as a covariate (figure 17).

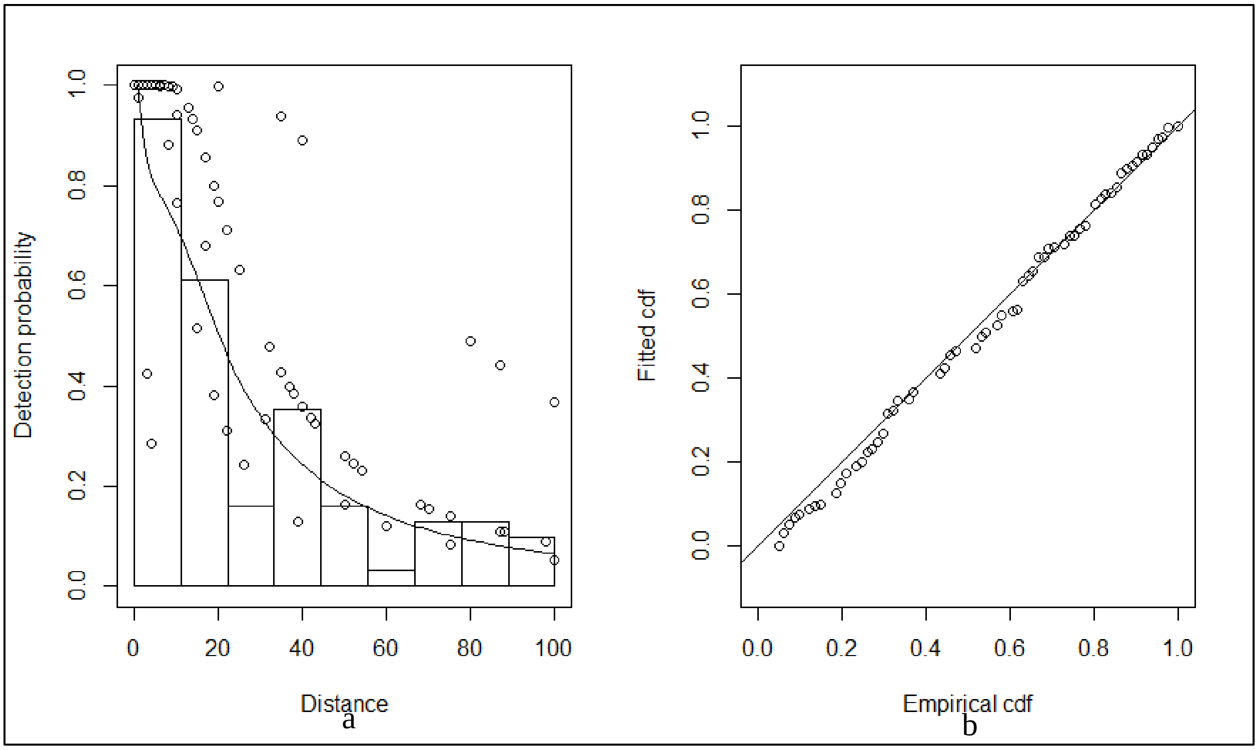

Figure 17. Detection Function for the Song of the Whale (ASI) Shipboard Surveys

Note: In figure 17, the fitted hazard rate detection function with month as a covariate (a) and associated Q-Q plot (b).

4.2 SPATIAL MODELS

Annual Models: The best unlimited model retained all covariates. It had the best deviance explained (34 percent) and lowest REML and AIC of all candidate models. Assessing model performance, the Q-Q plot was somewhat skewed at high values, but this was expected given the poor sampling at covariate extremes such as salinity and distance to shore (figure 18). Plots of residuals did not show evidence of systematic bias (figure 18).

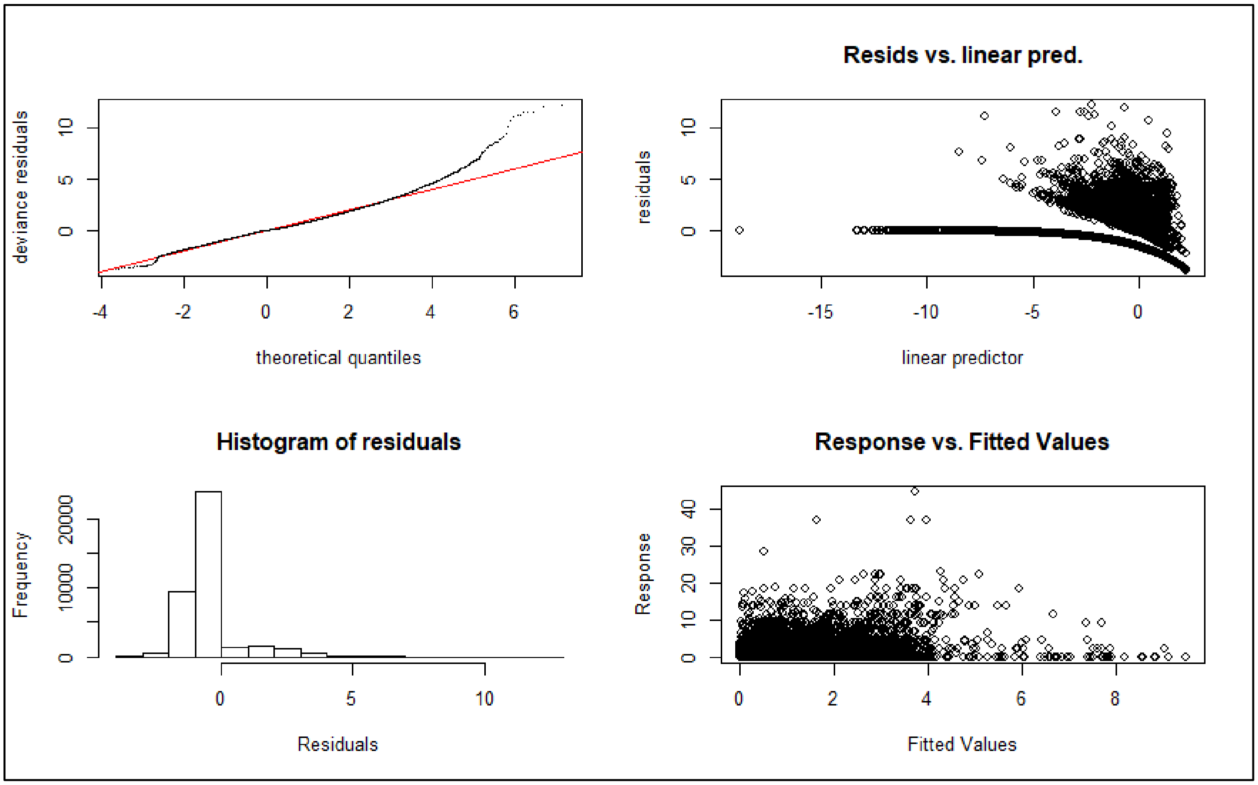

Figure 18. Q-Q Plot and Residual Analysis for the Best Annual Unlimited Model

Figure 19 shows the functional relationships to covariates fit by the model. Extreme values of chlorophyll a, depth, slope, and salinity were poorly sampled (see rug plots in figure 19) and had higher associated uncertainty, even though overall environmental extrapolation was low for annual models. Though most of the covariate relationships look relatively flat, there were many samples allowing for complex relationships to be fit. Small changes in covariate values can be significant. For dynamic covariates, there were apparent preferences for warmer temperatures, higher productivity, and lower salinity. The relationships with static covariates were less clear, but reviewing the predictions, there was higher predicted abundance in offshore areas.

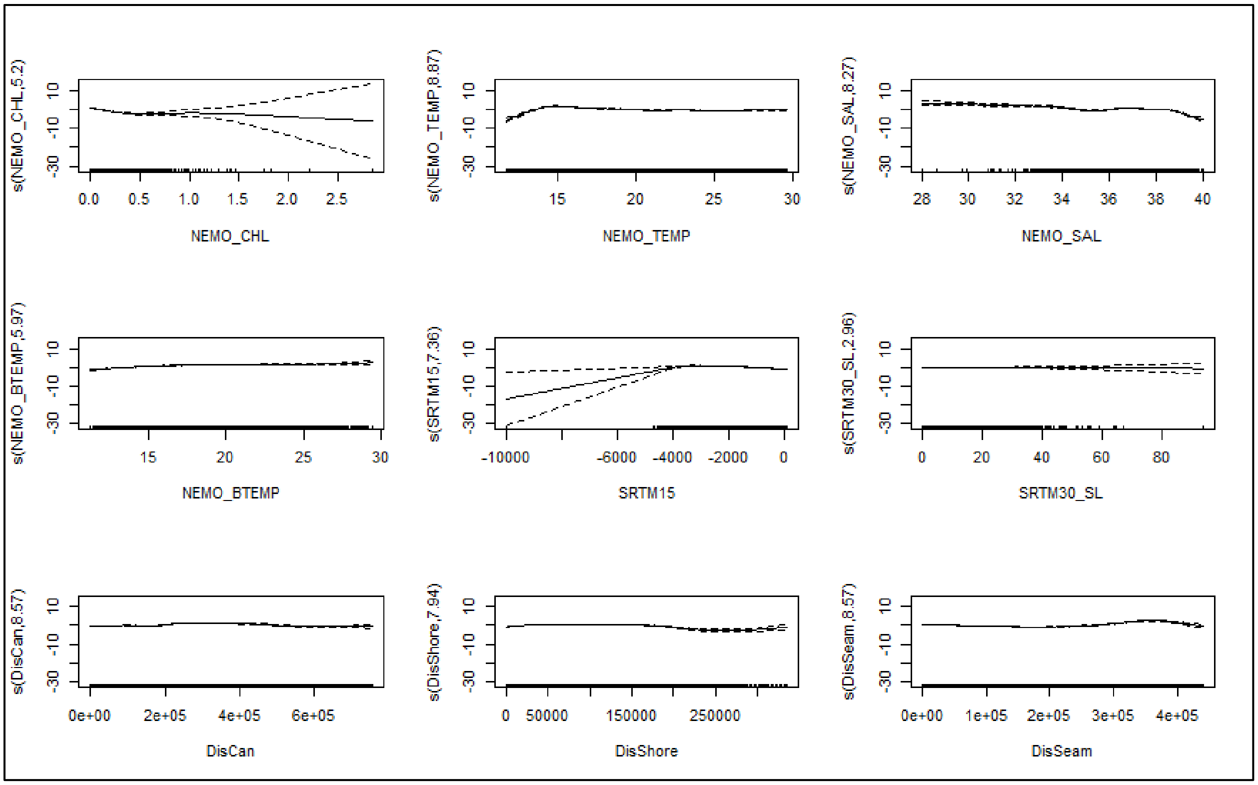

Figure 19. Functional Relationships of Covariates to Abundance for Best Annual Unlimited Model

Note: For figure 19, NEMO_CHL = Chlorophyll a; NEMO_TEMP = Sea Surface Temperature; NEMO_SAL = Salinity; NEMP_BTEMP = Bottom Temperature; SRTM15 = Bathymetry; SRTM30_SL = Slope; DisCan = Distance to Canyon; DisShore = Distance to Shore; and DisSeam = Distance to Seamount.

The best parsimonious model retained sea surface temperature, distance to canyon, distance to shore, and distance to seamount. It had the best deviance explained (28 percent) and lowest REML and AIC of all candidate models.

Figure 20 shows the functional relationships to covariates fit by the selected model. The U-shaped relationships for sea surface temperature and distance to seamount are difficult to interpret. It is unlikely these relationships represent different preferences of neritic versus oceanic turtles given the disparity in sightings and population numbers between those two groups and the physiological requirements of loggerhead sea turtles. It is more likely an artifact of limiting the wiggliness of the relationship than a true ecological relationship.

Distance to canyon and distance to shore showed more classical bell-shaped relationships, but they also are challenging to interpret ecologically. Spatial patterns of abundance and overall predicted abundance were similar to the unlimited model. Because of this, the lower deviance explained compared to the unlimited model, the limited amount of geographic extrapolation, and the difficult to interpret environmental relationships, This model was eliminated from consideration as the recommended model.

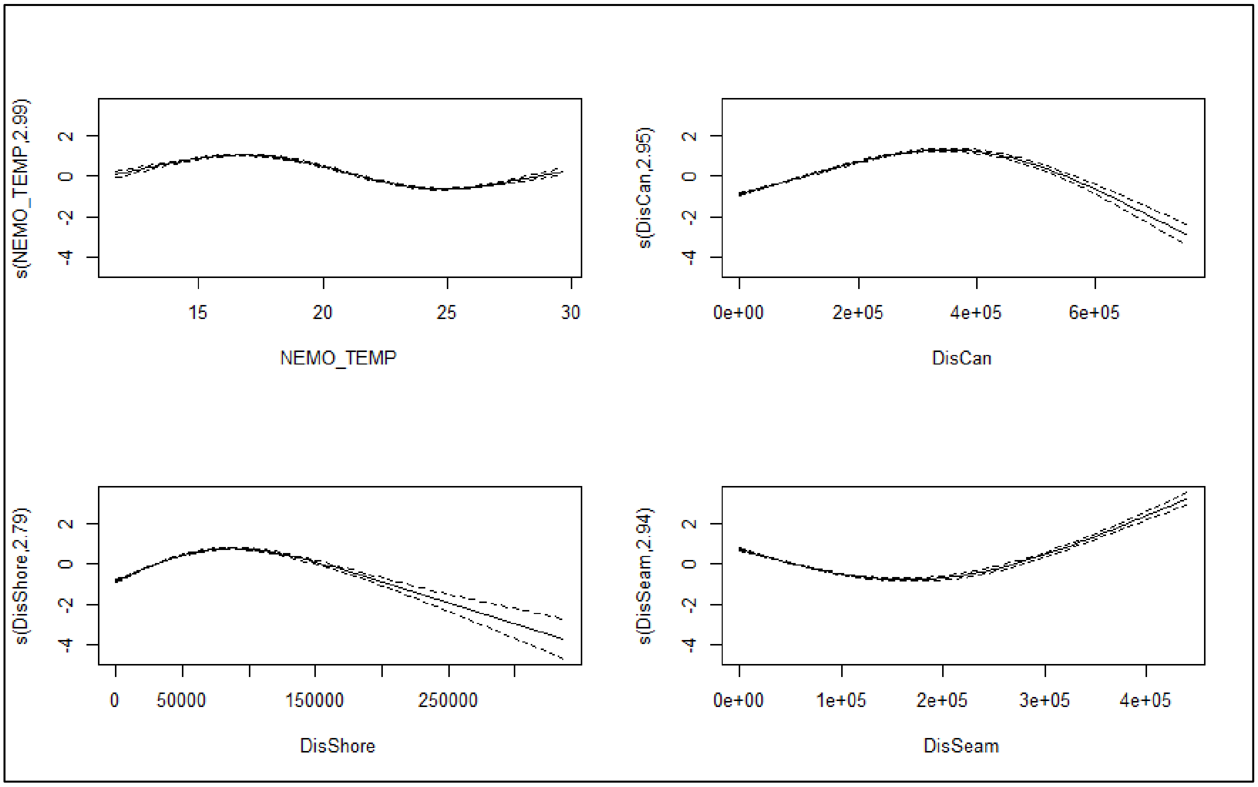

Figure 20. Functional Relationships of Covariates to Abundance for Best Annual Parsimonious Model

Note: For figure 20, NEMO_TEMP = Sea Surface Temperature; DisCan = Distance to Canyon; DisShore = Distance to Shore; and DisSeam = Distance to Seamount.

Seasonal models: Both unlimited and parsimonious models were attempted for the summer and winter seasons, using only segments from those seasons and the same methodology as the annual models, but limiting covariates to those that minimized environmental extrapolation.

The best summer model was the unlimited model, which retained all covariates. Sea surface temperature and distance to canyon were dropped prior to model fitting to limit environmental extrapolation. Deviance explained was 26 percent. This model was fit using 77 percent of the entire dataset and geographic extrapolation was 16 percent. Assessing model performance, the Q-Q plot was somewhat skewed at high values, but this was expected given the poor sampling at covariate extremes, such as salinity and distance to shore (figure 21), which were retained. Plots of residuals did not show evidence of systematic bias. Functional relationships were largely flat, and chlorophyll a, salinity, slope, and depth were poorly sampled at extreme values (figure 22).

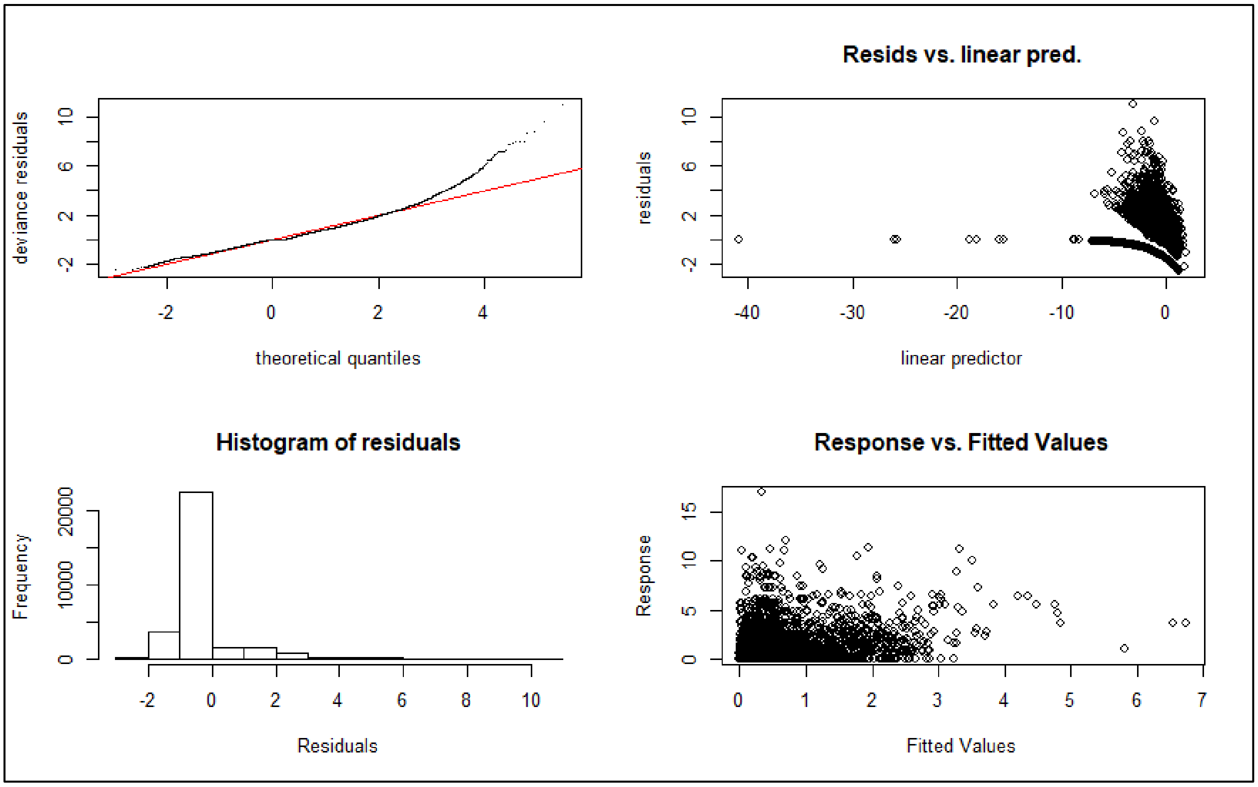

Figure 21. Q-Q Plot and Residual Analysis for the Best Summer Unlimited Model

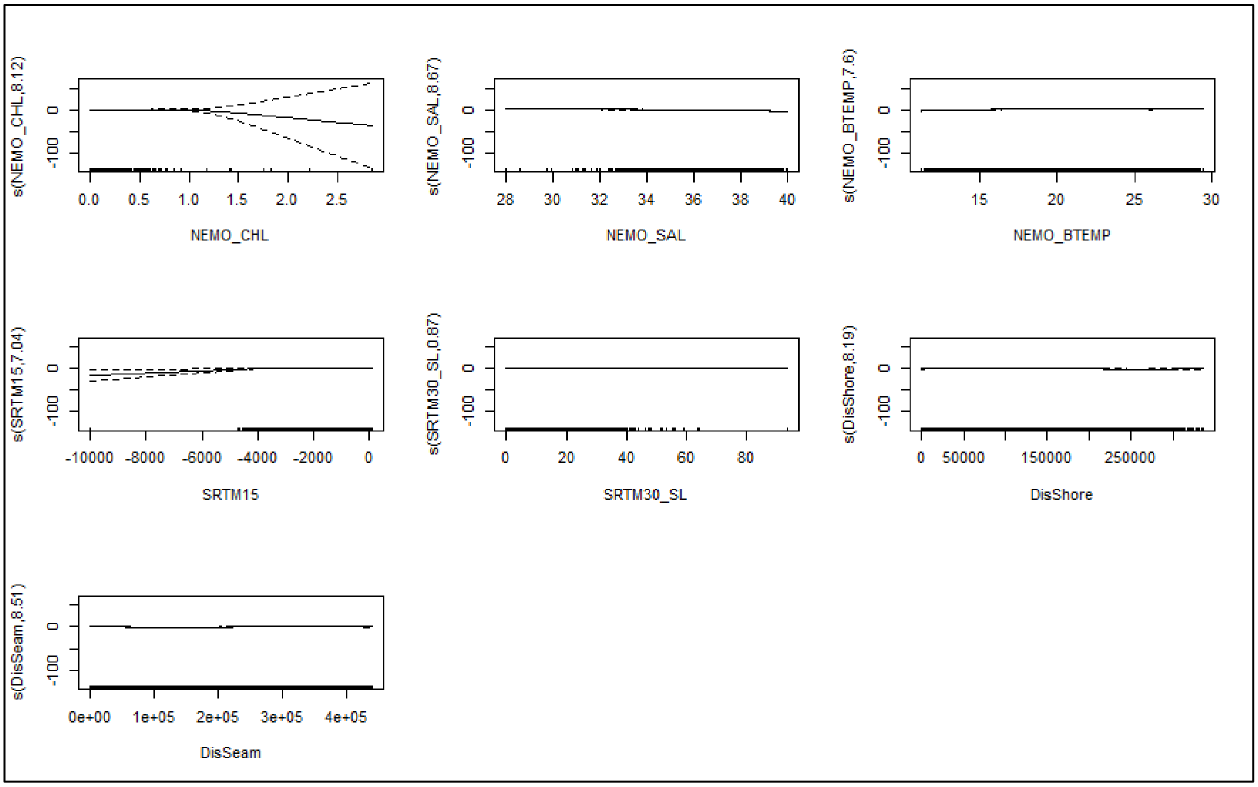

Figure 22. Functional Relationships of Covariates to Abundance for Best Summer Unlimited Model

Note: For figure 22, NEMO_CHL = Chlorophyll a; NEMO_SAL = Salinity; NEMP_BTEMP = Bottom Temperature; SRTM15 = Bathymetry; SRTM30_SL = Slope; DisShore = Distance to Shore; and DisSeam = Distance to Seamount.

Fitting a reasonable winter model was not possible. Available survey data in the winter was only 23 percent of the total dataset and was geographically limited, occurring mostly in the central Mediterranean Sea. While initial models seemed reasonable, there were runaway predictions with extremely high-density values (many orders of magnitude higher than any other grid cells) in some coastal areas. This was likely a combination of the largest availability bias adjustment occurring in the neritic zone in winter and extreme extrapolation. This occurred even when eliminating covariates that were the worst offenders for causing environmental extrapolation. This meant that the model was trying to predict the highest abundance in poorly sampled environments that contained many outlier values.

Possible solutions to combat these runaway predictions include limiting predicted density to the maximum value that was not extrapolated or by limiting the functional relationships themselves, but this was unsatisfying given the overall good performance of the annual model and the limited data in winter.

Because fitting a winter model was unsuccessful, using an annual average density is recommended, specifically the unlimited model, which is presented below. Seasonal models can be revisited if more winter surveys occur over a broader area or when there is more time to explore possible solutions.

4.3 PREDICTED DENSITY AND UNCERTAINTY

The total predicted abundance was 1,201,845 (CV=0.22; figure 23) for the annual unlimited model. The CV estimate includes both GAM parameter uncertainty and environmental variability. The abundance in the areas of geographic extrapolation was 192,826 (figure 23). The extent of geographic extrapolation was 16 percent, and the percent of the total predicted abundance that was in the geographic extrapolation areas was also 16 percent. The highest predicted densities were in the Southeastern Mediterranean off the coast of Egypt, the Northern Adriatic Sea, the Southern Algero-Provençal Basin, and the Tunisian Plateau. Predicted density was low in most coastal areas, the Aegean Sea, and the Eastern Mediterranean Sea (except for the hotspot off Egypt). Note that environmental covariates were poorly sampled close to shore, and there were many grid cells where predictions were not made within 5 to 10 km (3-6 mi) of shore. NUWC chose to not extrapolate the model into these unsampled grid cells as they were also poorly sampled by surveys. This is a source of underestimation of abundance in the model, though generally predicted density was lower close to shore and the missing cells represent 0.05 percent of the area of the Mediterranean Sea. If estimates are needed close to shore for management purposes, extrapolating values from nearby cells is recommended as the best solution. However, caution should be used when relying on estimates from individual cells for fine scale management. This is a broad scale model intended for basin-wide and regional density/abundance estimation and conservation action.

There were some extremely high values of CV (greater than 1) located around areas of low salinity, far distances to canyon, and extremely deep areas that were poorly sampled by surveys. For example, the Northern Adriatic Sea, the Libyan coast, and off the coast of Crete all had high values of CV (figure 24). Average CV was moderate (0.22) and was generally low in well-sampled areas, which was expected.

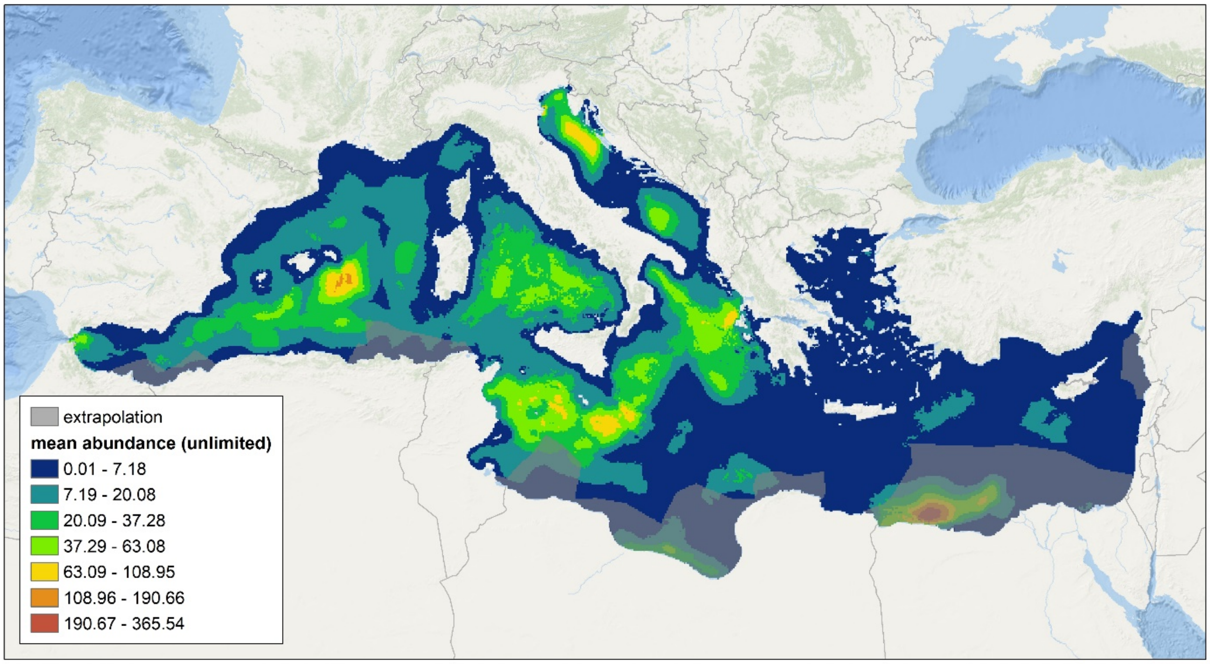

Figure 23. Abundance Prediction for the Unlimited Annual Model

Note: In figure 23, the prediction is an average of 192 monthly predictions. Units are in animals per 25 square km (9.6 square mi). Areas of geographical extrapolation are shaded grey.

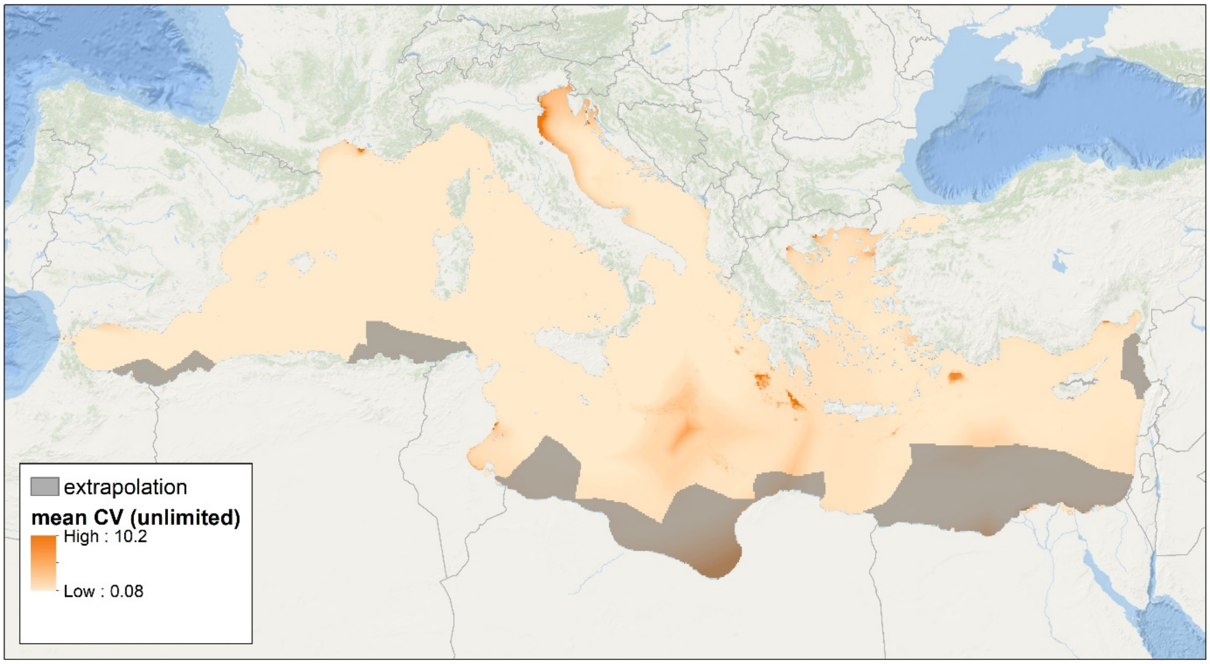

Figure 24. CV Prediction for the Unlimited Annual Model

Note: In figure 24, the CV is derived from 38,400 predictions (200 simulations for each month). Areas of geographical extrapolation are shaded grey.

Inter- and intra-annual variability were both high for abundance predictions (figure 25). Mean predicted abundance ranged from 3,600,000 to 560,000 in the monthly predictions. Predictions were high in winter and low in summer. The population abundance should not change this drastically between seasons, as the population is generally constrained within the Mediterranean Sea and does not migrate in and out seasonally.

The partial exceptions are juvenile turtles of Atlantic origin in the western basin that entrain in the Mediterranean Sea via the Strait of Gibraltar. These juvenile turtles come from two other loggerhead populations (Wallace et al. 2010) that can entrain in the Mediterranean Sea for 8 to 10 years (Carreras et al. 2006, Revelles 2007, and Eckert et al. 2008) and comprise a large percentage of the population of juvenile loggerheads in some Western Mediterranean regions. However, because they remain in the Mediterranean Sea for such long periods of time, one would not expect their entrance and departure from the Mediterranean to cause large seasonal changes in abundance.

This means that the intra-annual variability in NUWC’s predictions may be linked to the predicted relationships to environmental covariates and their seasonal changes, rather than seasonal changes in population abundance. Another possible explanation for the large predicted intra-annual variability is poor sampling in winter months. Because of this, it is recommended to use a single prediction over the entire study period, rather than seasonal averages, even though this may miss seasonal movement between the basins.

Fitting a simple linear trendline to the monthly abundance data, there was a slight downward trend in predicted abundance (figure 25) throughout the time of the collected survey data that was used for this study. The R2 value was only 0.04, so the trend was not strong. The best available data for the loggerhead population trends in the Mediterranean Sea came from counts of nesting females, which shows a slight increasing trend (Casale 2015 and Mazaris et al. 2017). Nesting females represent a small proportion of the total loggerhead population, so increasing nesting female populations and decreasing juvenile populations may be occurring concurrently. Juvenile loggerheads, which comprise most of the population, may be decreasing while nesting females are increasing. However, given the weak trend and no other evidence that the population is decreasing, the apparent downward trend in abundance may be an artifact of changing environmental conditions, as the predictions are based in part on environmental conditions, rather than actual population change.

More research is needed to determine if changes in population abundance are occurring, such as repeated, stratified density estimates covering the same area. This study, which combines multiple surveys over different time periods, geographic areas, and abundance varying with environmental covariates, is not the best study design for detecting trends.

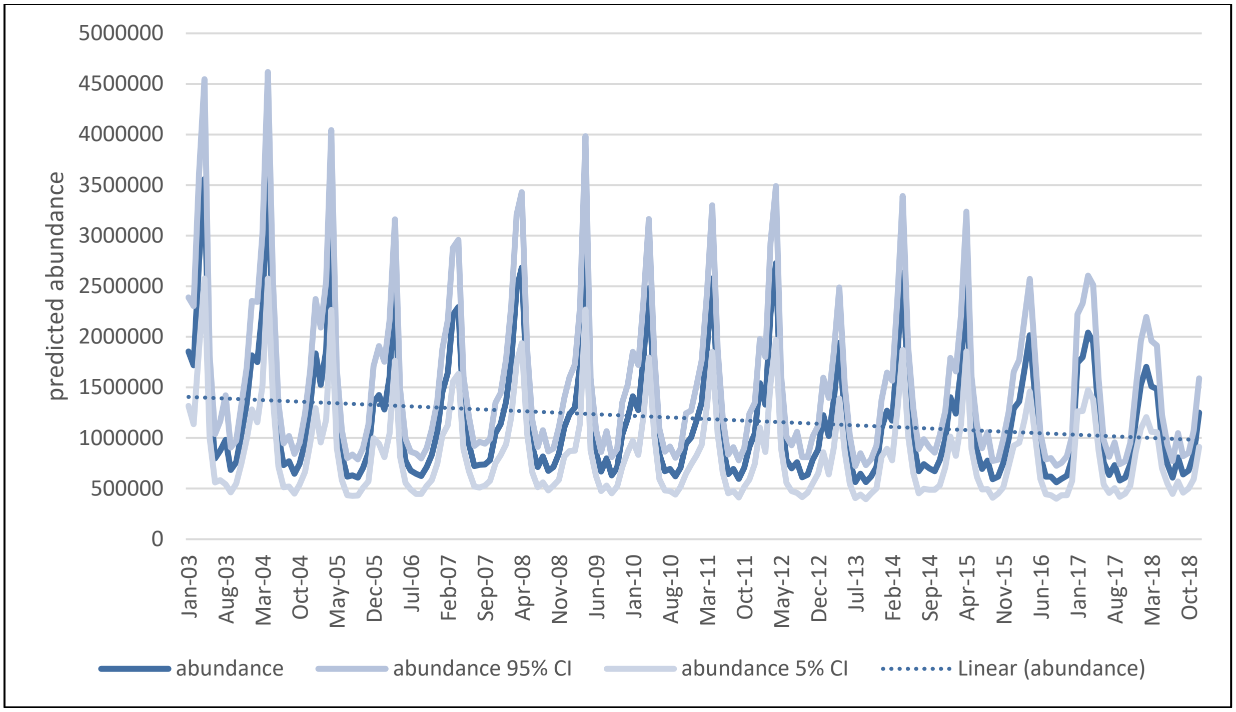

Figure 25. Monthly Abundance for the Unlimited Annual Model

Note: In figure 25, the 5 percent and 95 percent confidence interval (CI) values in this figure are based only on the GAM parameter uncertainty and do not include environmental variability and other sources of uncertainty. The trend line (dotted blue line) is a linear regression of mean abundance.

5. CONCLUSIONS

While most of the spatial density predictions appear reasonable based on the sightings data (figure 23) and satellite telemetry data from the region, the hotspot off Egypt is concerning given that there is no survey coverage in that area. The hotspot has the highest predicted density values in the model. Examining differences in the covariates in the hotspot versus the rest of the Eastern Mediterranean Sea, it appears that the high prediction is driven by distance to seamount, as the means of the other covariates were similar. The model predicts abundance increasing both close to and far from seamounts, which is challenging to interpret ecologically. Previous work by Fiori et al. (2016) found sea turtles to be attracted to seamounts.

Rabia and Attum (2015) found evidence of loggerheads stranding on the Egyptian coast, and Rabia and Attum (2020) observed sea turtles foraging in Lake Bardawil in Egypt. Additionally, the southern coast of the Eastern Mediterranean is a migratory corridor for turtles traveling from Cyprus to the East coast of Tunisia (Snape et al. 2016). Lastly, a recent shipboard survey (Panigada 2020) did detect two loggerhead sea turtles off the coast of Egypt. Despite this evidence that turtles are present in the waters off Egypt and migrate through the area, this hotspot should be treated with skepticism until a more formal density/abundance estimate can be made using line transect data. A model without the distance to seamount covariate was attempted, but it created more possible erroneous hotspots elsewhere. This bears more exploration in the future as the model appears to be sensitive to the inclusion of distance to seamount as a covariate.

With a few exceptions, the selected model predicted lower abundance in coastal and neritic areas, where large juveniles and adult turtles are known to forage, particularly in the Eastern Mediterranean. These neritic foraging areas have been confirmed by multiple lines of investigation (Casale 2018). Exceptions in this model were the Tunisian Plateau, the Northern Adriatic Sea, and the hotspot off Egypt. While most loggerheads in the Mediterranean Sea are juveniles (Casale and Heppell 2016), the model fails to show some important neritic foraging areas. The model can best be considered a model of oceanic loggerheads, which represent most loggerheads in the Mediterranean Sea. However, if this model is used for management purposes, some important segments of the population may be overlooked. Coupling this model with other data sources such as satellite telemetry and stable isotope analyses will be critical for holistic management of the loggerhead sea turtle population in the Mediterranean Sea.

Satellite telemetry data featured in the State of the World's Sea Turtle Report (SWOT Team 2019) showed loggerheads to be distributed almost throughout the entire Mediterranean Sea, though fewer locations were recorded in the North-central Mediterranean and Eastern Mediterranean. Higher densities of satellite telemetry data were found in the Alboran Sea, Tunisian Plateau, Adriatic Sea, and Tyrrhenian Sea. These areas of relatively higher and lower density of satellite telemetry location correlate well with the selected model's predicted density distribution, though caution must be taken when comparing spatial density models to density of satellite telemetry locations. There are significant biases associated with satellite telemetry, such as deployment bias, individual behavior, and the age classes tagged. Despite these biases, the SWOT Team (2019) report featured hundreds of tagged animals, and the general concurrence of the NUWC model and the tag data is good.

The model's population estimate can be compared to other population estimates from the region. Casale and Heppell (2016) presented a demographic model of the Mediterranean loggerhead sea turtle population based on the number of adult females, reproductive output, and assumptions about age of sexual maturity. That study represented a completely independent population estimate from its spatial density model. Casale and Heppell (2016) made three estimates of population, assuming age of sexual maturity at 21, 25, and 34 years old. The estimates were 1,197,087 (CI 805,658-1,732,765), 1,521,107 (CI 1,034,839-2,178,790), and 2,364,843 (CI 1,611,085-3,376,104) respectively. The selected model's population estimate of 1,201,845 (CV 0.22) was statistically similar (e.g., estimates overlapped when considering uncertainty) to the 21- and 25-year old scenarios but not the 34-year old scenario, though it is likely that the selected model is underestimating both abundance and its own uncertainty. This independent verification lends credence to both estimates as being valid.

Abundance estimates from the density predictions in the Adriatic Sea were similar to previously published density spatial models derived from the BWI ISPRA surveys (Fortuna et al.

2018). Both the Navy and Fortuna et al. (2018) models predicted high nearshore density in the Northeast Adriatic and the central Southern basin of the Adriatic. Predicted abundance was also statistically similar.

It is important to remember sources of potential bias in the selected model, even though the estimate is statistically similar to independent demographic population estimates. Possible sources of underestimation include the following: not accounting for perception bias, overestimating the amount of time animals are at the surface based on the depth at which dives were assumed to be started (3-4 m (10 to 13 ft) for dive data)), missing cells close to shore due to missing environmental covariates, and not detecting small animals. Aerial surveyors have indicated an ability to detect animals as small as 40 centimeters (16 inches) (Barco et al. 2018); however, animals of that size may be several years old already. Given the age structure of sea turtle populations, those missed animals represent a large fraction of the total population (Mazaris et al. 2005; Casale and Heppell 2016).

Possible sources of overestimation of population include the following: including sightings reported as hardshell turtles that may actually be green turtles and including the dive data from Spain that may be missing some surfacing events because the data were collected as average depths over five-minute time intervals. Overall, the model is probably underestimating density because missing small turtles is likely the largest effect, given the size of those age classes relative to the total population. Additionally, there are more sources of possible underestimation than overestimation. However, because the magnitude of these effects cannot be quantified, this is supposition only.

This spatial density model can be used by the Navy to estimate impacts to loggerhead sea turtles during its training and testing activities, and the model conforms to the requirements of the NMSDD. NUWC's hope is that it is useful for other marine spatial planning and conservation efforts in the Mediterranean Sea.

6. RECOMMENDATIONS

While the model presented here represents an excellent first attempt at a basin-wide spatial density model for the Mediterranean Sea and appears to match abundance estimates derived from demographic data, there are improvements that can be made.

There are additional survey data that could be added to the survey dataset, mostly from the University of Valencia as well as from new winter shipboard surveys in the Eastern Mediterranean associated with the ASI that were not available when this study was undertaken. The Eastern Mediterranean is data poor already, and winter surveys are a critical data gap. Inclusion of the new survey and any future surveys may allow winter models to be fit successfully.

Seasonal models could be explored in more depth to see if seasonal movements between the Eastern and Western basins can be captured. This will require either significantly more data in the winter season (and broader spatial coverage) or limiting winter predictions in some way to combat runaway extrapolation. As mentioned previously, while animals move between basins seasonally, the population would not be expected to vary significantly between seasons as all animals are either resident to the Mediterranean or entrain in the western basin for a significant period of time. The total abundance could also be limited to be equivalent in both seasons.

A major criticism of the selected model is that it is weighted heavily towards predicting the density distribution and abundance of oceanic juveniles at the expense of larger neritic turtles. While oceanic juveniles are the largest population segment, their importance, or lack thereof, in the selected model limits its use in management efforts that want to target adult populations and foraging areas. Two possible solutions exist, (1) fit separate models to neritic and deep areas, given that larger loggerhead sea turtles in the Mediterranean Sea spend most of their time in neritic waters (Mazor et al. 2016, review in Casale 2018), or (2) fit a single model to all the data but use a hierarchical GAM framework where one could include habitat as a factor (Pederson et al. 2019). Unfortunately, these options were outside the scope of this project.

Stratified availability bias estimates were used to better reflect changing dive behavior over time and space. However, a more complex treatment may be possible given the amount of available data. Modeling availability spatially in response to environmental covariates would allow for smooth relationships over time and space, unlike the current stratified estimates that have distinct boundaries spatially and temporally.

Lastly, it would be a major improvement to include more sources of uncertainty (e.g., dive data and detection function) in the model's overall estimate of CV. This should be possible given the initial results of the DenMod working group, but methods need to be peer-reviewed, published, and incorporated into R packages or otherwise be made available.

NUWC's ability to pursue any updates and improvements will depend on future funding. Research priorities will be dependent on available data, funder priorities, and available time.

7. BIBLIOGRAPHY

Barco, S.G., M.L. Burt, R.A. DiGiovanni Jr, W.M. Swingle, and A.S. Williard, "Loggerhead Turtle *Caretta caretta* Density and Abundance in Chesapeake Bay and the Temperate Ocean Waters of the Southern Portion of the Mid-Atlantic Bight," Endangered Species Research, 37, 2018, pp. 269-–287.

Becker, E.A., K.A. Forney, D.G. Foley, R.C. Smith, T.J. Moore, and J. Barlow, "Predicting Seasonal Density Patterns of California Cetaceans Based on Habitat Models," Endangered Species Research, 23, 2014, pp. 1–22.

Becker, J.J., D.T. Sandwell, W.H.F. Smith, J. Braud, B. Binder, J. Depner, D. Fabre, J. Factor, S. Ingalls, S-H. Kim, R. Ladner, K. Marks, S. Nelson, A. Pharaoh, R. Trimmer, J. Von Rosenberg, G. Wallace, and P. Weatherall, "Global Bathymetry and Elevation Data at 30 Arc Seconds Resolution: SRTM30_PLUS," Marine Geodesy, 32 (4), 2009, pp. 355–371.

Behrenfeld, M.J. and P.G. Falkowski, "Photosynthetic Rates Derived from Satellite-Based Chlorophyll Concentration," Limnology and Oceanography, 42, 1997, pp. 1–20.

Bolten, A.B., "Variation in Sea Turtle Life History Patterns: Neritic vs. Oceanic Developmental Stages," In: Lutz, P.L., J.A. Musick, and J. Wyneken (eds.), *Biology of Sea Turtles*, vol. II, CRC Press, Boca Raton, FL, 2003, pp. 243–257.

Bouchet, P., D.L. Miller, J.J. Roberts, L. Mannocci, C.M. Harris, and L. Thomas, "From Here and Now to There and Then: Practical Recommendations for Extrapolating Cetacean Density Surface Models to Novel Conditions," *CREEM Technical Report 2019-01*, Centre for Research into Ecological & Environmental Modelling (CREEM), University of St Andrews, 2019, p. 59.

Broderick, A.C., M.S. Coyne, W.J. Fuller, F. Glen, and B.J. Godley, "Fidelity and Over-Wintering of Sea Turtles," *Proceedings of the Royal Society B*, 274, 2007, pp. 1533−1538.

Buckland, S.T., D.R. Anderson, K.P. Burnham, J.L. Laake, D.L. Borchers, and L. Thomas, *Introduction to Distance Sampling*. Oxford University Press, New York, 2001.

Bureau of Ocean Energy Management, "Atlantic Marine Assessment Program for Protected Species: 2010-2014 (OCS Study BOEM 2017-071)," U.S. Dept. of the Interior, Bureau of Ocean Energy Management, Washington, DC, 2017, https://www.boem.gov/espis/5/5638.pdf .

Cañadas, A., private communication, 10 June 2019.

Cañadas, A. and J.A. Vázquez, "Conserving Cuvier's Beaked Whales in the Alboran Sea (SW Mediterranean): Identification of High Density Areas to be Avoided by Intense Man-Made Sound," *Biological Conservation*, 178, 2014, pp. 155–162.

Cardona, L. and G.C. Hays, "Ocean Currents, Individual Movements and Genetic Structuring of Populations," *Marine Biology*, 165, 2018, p. 10.

Carreras, C., C. Monzón-Argüello, L.F. López-Jurado, P. Calabuig, J.J. Bellido-Lopez, J.J. Castillo, P. Sánchez, P. Medina, J. Tomás, P. Gozalbes, G. Fernandez, A. Marco, and L. Cardona, "Origin and Dispersal Routes of Foreign Green and Kemp's Ridley Turtles in Spanish Atlantic and Mediterranean Waters," *Amphibia-Reptilia*, 35, 2014, pp. 73−86.

Carreras, C., S. Pont, F. Maffucci, M. Pascual, A. Barceló, F. Bentivegna, L. Cardona, F. Alegre, M. SanFélix, G. Fernandez, and A. Aguilar, "Genetic Structuring of Immature Loggerhead Sea Turtles (*Caretta caretta*) in the Mediterranean Sea Reflects Water Circulation Patterns," *Marine Biology*, 149, 2006, pp. 1269−1279.

Carreras, C., M. Pascual, L. Cardona, A. Marco, J.J. Bellido-Lopez, J.J. Castillo, J. Tomás, J.A. Raga, M. Sanfélix, G. Fernandez, and A. Aguilar, “Living Together but Remaining Apart: Atlantic and Mediterranean Loggerhead Sea Turtles (*Caretta caretta*) in Shared Feeding Grounds,” *Journal of Heredity*, 102, 2011, pp. 666−677.

Carretta, J.V., M.S. Lowry, C.E. Stinchcomb, M.S. Lynn, and R.E. Cosgrove, “Distribution and Abundance of Marine Mammals at San Clemente Island and Surrounding Offshore Waters: Results from Aerial and Ground Surveys in 1998 and1999,” NOAA Administrative Report LJ-00-02, 2000.

Casale, P., “*Caretta caretta* (Mediterranean Subpopulation)” The IUCN Red List of Threatened Species 2015, e.T83644804A83646294, 2015, https://dx.doi.org/10.2305/IUCN.UK.2015-4.RLTS.T83644804A83646294.en .

Casale, P. and S.S. Heppell, “How Much Sea Turtle ByCatch is too Much? A Stationary Age Distribution Model for Simulating Population Abundance and Potential Biological Removal in the Mediterranean,” *Endangered Species Research*, 29, 2016, pp. 239–254.

Casale, P. and D. Margaritoulis, eds., *Sea Turtles in the Mediterranean: Distribution, Threats and Conservation Priorities*, Gland, Switzerland, IUCN, 2010.

Casale, P. and P. Mariani, “The First ‘Lost Year’ of Mediterranean Sea Turtles: Dispersal Patterns Indicate Subregional Management Units for Conservation,” *Marine Ecology Progress Series*, 498, 2014, pp. 263−274.

Casale, P. and A.D. Tucker, “*Caretta caretta* (amended version of 2015 assessment),” The IUCN Red List of Threatened Species 2017: e.T3897A119333622, 2017, https://dx.doi.org/10.2305/IUCN.UK.2017-2.RLTS.T3897A119333622.en .

Casale, P., P. Nicolosi, D. Freggi, M. Turchetto, and R. Argano, “Leatherback Turtles (*Dermochelys coriacea*) in Italy and in the Mediterranean Basin,” *Herpetological Journal*, 13, 2003, pp. 135−139.

Casale, P., A.C. Broderick, J.A. Camiñas, L. Cardona, C. Carreras, A. Demetropoulos, W.J. Fuller, B.J. Godley, S. Hochscheid, Y. Kaska, B. Lazar, D. Margaritoulis, A. Panagopoulou, A.L.F. Rees, J. Tomás, and O. Türkozan, “Mediterranean Sea Turtles: Current Knowledge and Priorities for Conservation and Research,” *Endangered Species Research*, 36, 2018, pp. 229–267.

Chimienti M., M.F. Blasi, and S. Hochscheid, “Movement Patterns of Large Juvenile Loggerhead Turtles in the Mediterranean Sea: Ontogenetic Space use in a Small Ocean Basin,” *Ecology and Evolution*, 00, 2020, pp. 1–15.

Clusa, M., C. Carreras, M. Pascual, S.J. Gaughran, S. Piovano, C. Giacoma, G. Fernandez, Y. Levy, J. Tomás, J.A. Raga, F. Maffucci, S. Hochscheid, A. Aguilar, and L. Cardona, “Fine-Scale Distribution of Juvenile Atlantic and Mediterranean Loggerhead Turtles (*Caretta caretta*) in the Mediterranean Sea,” *Marine Biology*, 161, 2014, pp. 509−519.

Eckert, S.A., J.E. Moore, D.C. Dunn, R.S. van Buiten, K.L. Eckert, and P.N. Halpin, “Modeling Loggerhead Turtle Movement in the Mediterranean: Importance of Body Size and Oceanography,” *Ecological Applications*, 18, 2008, pp. 290−308.

Elith, J., M. Kearney, and S. Phillips, “The Art of Modelling Range-Shifting Species,” *Methods in Ecology and Evolution*, 1(4), 2010, pp. 330–342.

Fiori, C., L. Giancardo, M. Aïssi, J. Alessi, and P. Vassallo, “Geostatistical Modelling of Spatial Distribution of Sperm Whales in the Pelagos Sanctuary Based on Sparse Count Data and Heterogeneous Observations,” *Aquatic Conservation: Marine and Freshwater Ecosystems*, 24(3–4), 2014, pp. 41–49.

Fiori, C., C. Paoli, J. Alessi, A. Mandich, and P. Vassallo, “Seamount Attractiveness to Top Predators in the Southern Tyrrhenian Sea (Central Mediterranean),” *Journal of the Marine Biological Association of the United Kingdom*, 96(3), 2016, pp. 769–775.

Forcada, J., M. Gazo, A. Aguilar, J. Gonzalvo, and M. Fernández-Contreras, “Bottlenose Dolphin Abundance in the NW Mediterranean: Addressing Heterogeneity in Distribution,” *Marine Ecology Progress Series*, 275, 2004, pp. 275–287.

Foster, S.D. and M.V. Bravington, “A Poisson–Gamma Model for Analysis of Ecological Non-Negative Continuous Data,” *Environmental and Ecological Statistics*, 20, 2013, pp. 533–552.

Fortuna, C.M., D. Holcer, and P. Mackelworth, “Conservation of Cetaceans and Sea Turtles in the Adriatic Sea: Status of Species and Potential Conservation Measures,” *IPA Adriatic Cross-border Cooperation Programme*, 2015.

Fortuna, C. M., A. Cañadas, D. Holcer, B. Brecciaroli, G.P. Donovan, B. Lazar, G. Mo, L. Tunesi, and P.C. Mackelworth, “The Coherence of the European Union Marine Natura 2000 Network for Wide-Ranging Charismatic Species: A Mediterranean Case Study,” *Frontiers in Marine Science*, vol. 5. DOI=10.3389/fmars.2018.00356, 2018.

Fuentes, M.M.P.B., I. Bell, R. Hagihara, M. Hamann, J. Hazel, A. Huth, J.A. Seminoff, S. Sobtzick, and H. Marsh, “Improving In-Water Estimates of Marine Turtle Abundance by Adjusting Aerial Survey Counts for Perception and Availability Biases,” *Journal of Experimental Marine Biology and Ecology*, 471, 2015, PP. 77–83.

Gómez de Segura, A., J. Tomás, S.N. Pedraza, E.A. Crespo, and J.A. Raga, “Abundance and Distribution of the Endangered Loggerhead Turtle in Spanish Mediterranean Waters and the Conservation Implications,” *Animal Conservation*, 9, 2006, pp. 199–206.

Hochscheid, S., F. Bentivegna, M.N. Bradai, and G.C. Hays, “Overwintering Behaviour in Sea Turtles: Dormancy is Optional,” *Marine Ecology Progress Series*, 340, 2007, pp. 287−298.

Hochscheid, S., F. Bentivegna, A. Hamza, and G.C. Hays, “When Surfacers do not Dive: Multiple Significance of Extended Surface Times in Marine Turtles,” *Journal of Experimental Biology*, 213, 2010, pp. 1328−1337.

Hochscheid S., A. Travaglini, F. Maffucci, G.C. Hays, and F. Bentivegna, "Since Turtles Cannot Talk: What Beak Movement Sensors Can Tell us About the feeding Ecology of Neritic Loggerhead Turtles, *Caretta caretta*," *Marine Ecology*, 34(3), 2013, pp. 321–333.

Hochscheid, S., "Why We Mind Sea Turtles' Underwater Business: A Review on the Study of Diving Behavior," *Journal of Experimental Marine Biology and Ecology*, 450, 2014, pp. 118–136.

Hochscheid, S., "The Datasets Generated During and/or Analyzed During the Current Study are Available in the Movebank Data Repository," 2020, https://doi.org/10.5441/001/1.1f1h87r8 .

Howell, E.A., A. Hoover, S.R. Benson, H. Bailey, J.J. Polovina, J.A. Seminoff, and P.H. Dutton, "Enhancing the TurtleWatch Product for Leatherback Sea Turtles, a Dynamic Habitat Model for Ecosystem-Based Management," *Fisheries Oceanography*, 24, 2015, pp. 57–68.

IHO-IOC Commission, "*The IHO-IOC GEBCO Cook Book*," vol. 103, p. 416, Monaco: IHO Publication B-11, IOC Manuals and Guides 63, France, September 2018, p. 429.

Laake, J., J. Calambokidis, S. Osmek, and D. Rugh, "Probability of Detecting Harbor Porpoise from Aerial Surveys: Estimating g(0)," *The Journal of Wildlife Management*, 61(1), 1997, pp. 63–75.

Lazzari, P., C. Solidoro, V. Ibello, S. Salon, A. Teruzzi, K. Béranger, S. Colella, and A. Crise, "Seasonal and Inter-Annual Variability of Plankton Chlorophyll and Primary Production in the Mediterranean Sea: A Modelling Approach," *Biogeosciences*, 9, 2012, pp. 217–233.

Longhurst, A.R., *Ecological Geography of the Sea*, Oxford, Academic Press, 2007.

Mannocci, L., J.J. Roberts, P.N. Halpin, M. Authier, O.J. Boisseau, M.N. Bradai, A. Cañadas, C.A. Chicote, L. David, N. Di-Meglio, C.M. Fortuna, A. Frantzis, M. Gazo, T. Genov, P.S. Hammon, D. Holcer, K. Kaschner, D. Kerem, G. Lauriano, T. Lewis, G.N. di Sciara, S. Panigada, J.A. Raga, A. Scheinin, V. Ridoux, A. Vella, and J.G. Vella, "Assessing Cetacean Surveys Throughout the Mediterranean Sea: A Gap Analysis in Environmental Space," *Scientific Reports*, 8(3126), 2018 (a), pp. 1–14.

Mannocci L., J.J. Roberts, and P.N. Halpin, "Development of Exploratory Marine Species Density Models in the Mediterranean Sea," final report, Report prepared for Naval Facilities Engineering Command, Atlantic, under Contract No. N62470-15-D-8006, Task Order TO37, Duke University Marine Geospatial Ecology Laboratory, Durham, NC, March 2018 (b).

Marine Turtle Specialist Group, "Marine Turtle Red List Assessments," May 2020, https://www.iucn-mtsg.org/statuses .

Marques, F. F. C., and S. T. Buckland, "Covariate Models for the Detection Function," Buckland, S.T., D.R. Anderson, K.P. Burnham, J.L. Laake, D.L. Borchers, and L. Thomas, eds., *Advanced Distance Sampling*, Oxford, United Kingdom: Oxford University Press, 2004, pp. 31–47.

Marques, T.A., L. Thomas, S.G. Fancy, and S.T. Buckland, “Improving Estimates of Bird Density using Multiple Covariate Distance Sampling,” *The Auk*, 124(4), 2007, pp. 1229–1243.

Mazaris, A.D., Ø. Fiksen, and Y.G. Matsinos, “Using an Individual-Based Model for Assessment of Sea Turtle Population Viability,” *Population Ecology*, 47, 2005, pp. 179–191.

Mazaris, A.D., G. Schofield, C. Gkazinou, V. Almpanidou, and G.C. Hays, “Global Sea Turtle Conservation Successes,” *Science Advances*, 3:e1600730, 2017, pp. 1–7.

Mazor, T., M. Beger, J. McGowan, H.P. Possingham, and S. Kark, “The Value of Migration Information for Conservation Prioritization of Sea Turtles in the Mediterranean,” *Global Ecology and Biogeography*, 25, 2016, pp. 540−552.

Mesgaran, M., R.D. Dousens, and B. Webber, “Here Be Dragons: A Tool for Quantifying Novelty due to Covariate Range and Correlation Change when Projecting Species Distribution Models,” *Diversity and Distributions*, 20, 2014, 1147–1159.

Miller, D.L., M.L. Burt, E.A. Rexstad, and L. Thomas, “Spatial Models for Distance Sampling Data: Recent Developments and Future Directions,” *Methods in Ecology and Evolution*, 4, 2013, pp. 1001–1010.

Mrosovsky, N., “Thermal Biology of Sea Turtles,” *American Zoologist*, 20(3), 1980, pp. 531–547.

Mussi, B., A. Miragliuolo, A. Zucchini, and D.S. Pace, “Occurrence and Spatio-Temporal Distribution of Sperm Whale (*Physeter macrocephalus*) in the Submarine Canyon of Cuma (Tyrrhenian Sea, Italy),” *Aquatic Conservation: Marine and Freshwater Ecosystems*, 24(S1), 2014, pp. 59–70.

National Oceanographic and Atmospheric Administration, “Global Self-Consistent Hierarchical High-Resolution Geography,” ver. 2.3.5, released 12 April 2016, distributed under the Lesser GNU Public License, 2016.

Oceanographic Turtles Project, “SOCIB/Oceanographic Turtles,” May 2020, www.socib.es/tortugas .

Olson, C.J., J.J. Becker, and D.T. Sandwell, “SRTM15_PLUS: Data Fusion of Shuttle Radar Topography Mission (SRTM) Land Topography with Measured and Estimated Seafloor Topography,” NCEI Accession 0150537, 2016.

Panigada, S., private communication, 11 May 2020.

Panigada, S. and A. Cañadas, private communication 29 July 2019.

Pedersen, E.J., D.L. Miller, G.L. Simpson, and N. Ross, “Hierarchical Generalized Additive Models in Ecology: an introduction with mgcv,” PeerJ, 7:e6876, 2019, pp. 1–42.

Pollock, K.H., H.D. Marsh, I.R. Lawler, and M.W. Alldredge, "Estimating Animal Abundance in Heterogeneous Environments: An Application to Aerial Surveys for Dugongs," *The Journal of Wildlife Management*, 70, 2006, pp. 255–262.

Populus, J., M. Vasquez, J. Albrecht, E. Manca, S. Agnesi, Z. Al Hamdani, J. Andersen, A. Annunziatellis, T. Bekkby, A. Bruschi, V. Doncheva, V. Drakopoulou, G. Duncan, R. Inghilesi, C. Kyriakidou, F. Lalli, H. Lillis, G. Mo, M. Muresan, M. Salomidi, D. Sakellariou, M. Simboura, A. Teaca, D. Tezcan, V. Todorova, and L. Tunesi, "A European Broad-Scale Seabed Habitat Map," EUSeaMap, 2017, https://doi.org/10.13155/49975 .

Rabia, B. and O. Attum, "Distribution and Status of Sea Turtle Nesting and Mortality Along the North Sinai Coast, Egypt (*Reptilia: Cheloniidae*)," *Zoology in the Middle East*, 61(1), 2015, pp. 26–31.

Rabia, B. and O. Attum, "Sea Turtles in Lake Bardawil, Egypt - Size Distribution and Population Structure," *The Herpetological Bulletin*, 151, 2020, pp. 32–36.

Revelles, M., L. Cardona, A. Aguilar, M. San Felix, and G. Fernandez, "Habitat use by Immature Loggerhead Sea Turtles in the Algerian Basin (Western Mediterranean): Swimming Behaviour, Seasonality and Dispersal Pattern," *Marine Biology*, 151, 2007, pp. 1501−1515.

Revelles, M., J.A. Camiñas, L. Cardona, M.L. Parga, J. Tomás, A. Aguilar, F. Alegre, J.A. Raga, A. Bertolero, and G. Oliver, "Tagging Reveals Limited Exchange of Immature Loggerhead Sea Turtles (*Caretta Caretta*) Between Regions in the Western Mediterranean," *Scientia Marina*, 72, 2008, pp. 511−518.

Revuelta, O., C. Carreras, F. Domènech, P. Gozalbes, J. Tomás, "First Report of an Olive Ridley (*Lepidochelys Olivacea*) in the Mediterranean Sea," *Mediterranean Marine Science*, 16, 2015, pp. 346−351.

Roberts, J.J., B.D. Best, D.C. Dunn, E.A. Treml, and P.N. Halpin, "Marine Geospatial Ecology Tools: An Integrated Framework for Ecological Geoprocessing with ArcGIS, Python, R, MATLAB, and C++," *Environmental Modelling & Software*, 25, 2010, pp. 1197–1207.

Roberts, J.J., L. Mannocci, R.S. Schick, and P.N. Halpin, "Final Project Report: Marine Species Density Data Gap Assessments and Update for the AFTT Study Area, 2017-2018 (Opt. Year 2)," Document version 1.0, Report prepared for Naval Facilities Engineering Command, Atlantic, Duke University Marine Geospatial Ecology Laboratory, Durham, NC, 2018.

Seminoff, J.A., "*Chelonia mydas*," The IUCN Red List of Threatened Species 2004: e.T4615A11037468, 2004, https://dx.doi.org/10.2305/IUCN.UK.2004.RLTS.T4615A11037468.en .

Simoncelli, S., C. Fratianni, N. Pinardi, A. Grandi, M. Drudi, P. Oddo, and S. Dobricic, "Mediterranean Sea Physical Reanalysis (CMEMS MED-Physics) [Dataset]," Copernicus Monitoring Environment Marine Service (CMEMS), 2019, https://doi.org/10.25423/MEDSEA_REANALYSIS_PHYS_006_004 .

Snape, R.T.E., A.C. Broderick, B.A. Çiçek, W.J. Fuller, F. Glen, K. Stokes, and B.J. Godley, "Shelf Life: Neritic Habitat use of a Turtle Population Highly Threatened by Fisheries," *Diversity and Distribution*, 22, 2016, pp. 797−807.

Society for the Protection of Turtles, "Loggerhead Sea Turtle Dive data from Cyprus," unpublished data, 2020.

SWOT Team, "State of the World's Turtles Report," vol. 14, 2019, https://www.seaturtlestatus.org/swot-report-vol-14 .

Tepsich, P., M. Rosso, P.N. Halpin, and A. Moulins, "Habitat Preferences of Two Deep-Diving Cetacean Species in the Northern Ligurian Sea," *Marine Ecology Progress Series*, 508, 2014, pp. 247–260.

Teruzzi, A., G. Bolzon, G. Cossarini, P. Lazzari, S. Salon, A. Crise, and C. Solidoro, "Mediterranean Sea Biogeochemical Reanalysis (CMEMS MED-Biogeochemistry) [Dataset]," Copernicus Monitoring Environment Marine Service (CMEMS), 2019, https://doi.org/10.25423/MEDSEA_REANALYSIS_BIO_006_008 .

Tomás, J. and J. Raga, "Occurrence of Kemp's Ridley Sea Turtle (*Lepidochelys Kempii*) in the Mediterranean," *Marine Biodiversity Records*, 1: e58, 2008, pp. 1–2.

Wallace B.P., A.D. DiMatteo, B.J. Hurley, E.M. Finkbeiner, A.B. Bolten, M.Y. Chaloupka, B.J. Hutchinson, A. Abreu, D. Amorocho, K.A. Bjorndal, J. Bourjea, B.W. Bowen, R. Briseno, P. Casale, B.C. Choudhury, A. Costa, P.H. Dutton, A. Fallabrino, A. Girard, M. Girondot, M. Godfrey, M. Hamann, M. López-Mendilaharsu, M.A. Marcovaldi, J. Mortimer, J.A. Musick, R. Nel, N.J. Pilcher, J.A. Seminoff, S. Troëng, B. Witherington, R. Mast, "Regional Management Units for Marine Turtles: A Novel Framework for Prioritizing Conservation and Research Across Multiple Scales, *PLOS ONE*, 5(12): e15465, 2010, pp. 1–11.

Wood, S.N., "Thin-Plate Regression Splines," *Journal of the Royal Statistical Society B*, 65(1), 2003, pp. 95–114.

Wood, S.N., "Fast Stable Restricted Maximum Likelihood and Marginal Likelihood Estimation of Semiparametric Generalized Linear Models," *Journal of the Royal Statistical Society B*, 73(1), 2011, pp. 3–36.

Wurtz, M. and M. Rovere, *Atlas of the Mediterranean Seamounts and Seamount-Like Structures*, Gland, Switzerland and Malaga, Spain: IUCN, 2015.

APPENDIX
SURVEY EFFORT BY MONTH

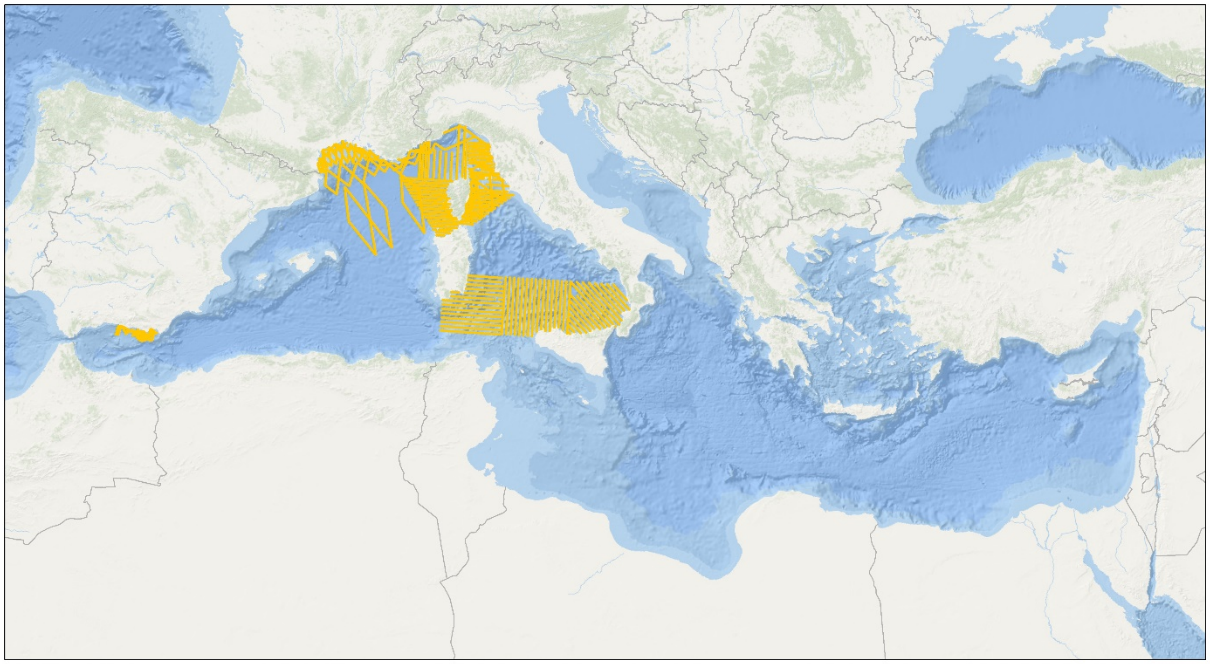

Figure A-1. Available Survey Effort for the Month of January

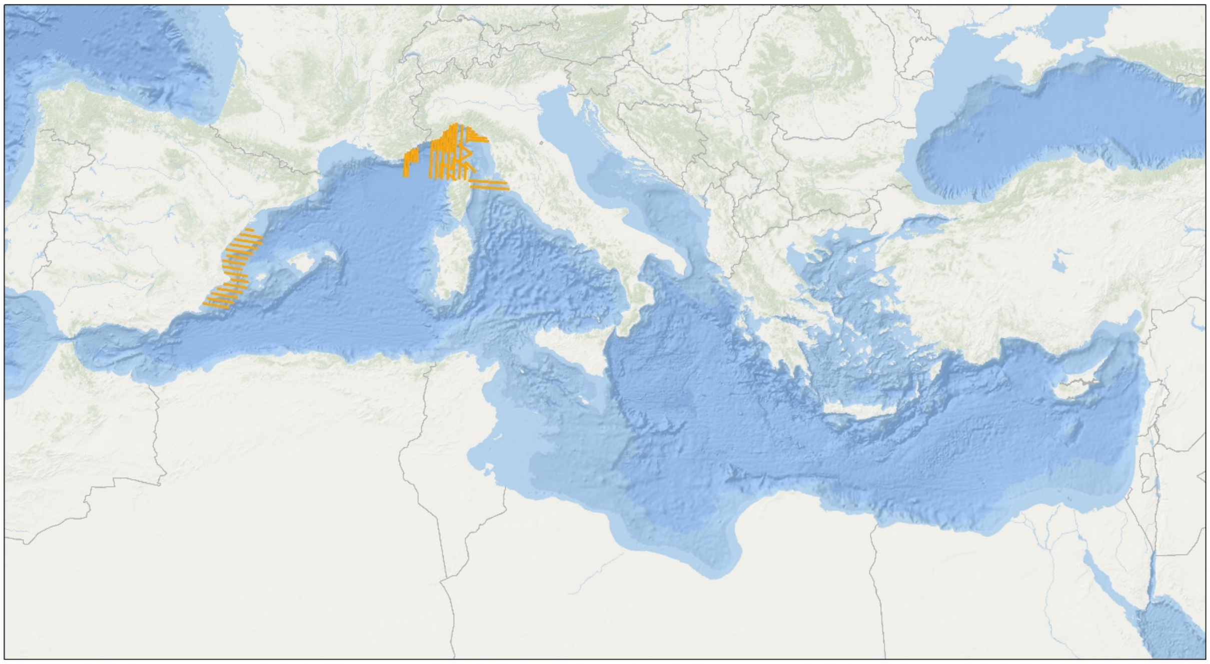

Figure A-2. Available Survey Effort for the Month of February

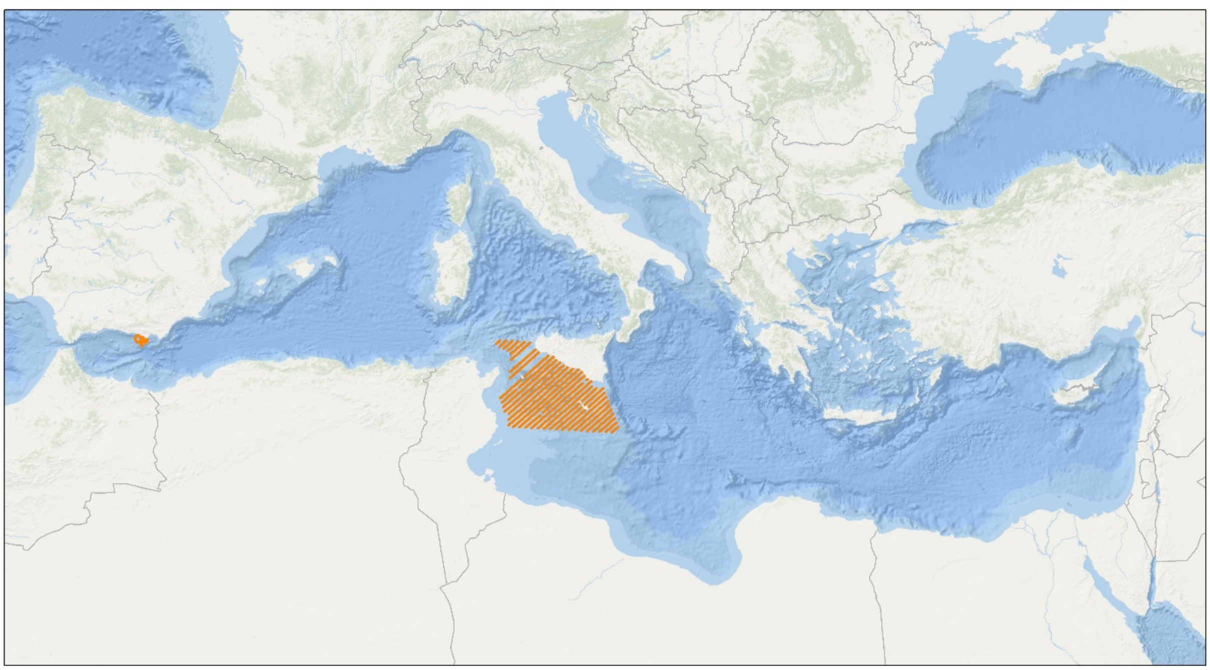

Figure A-3. Available Survey Effort for the Month of March

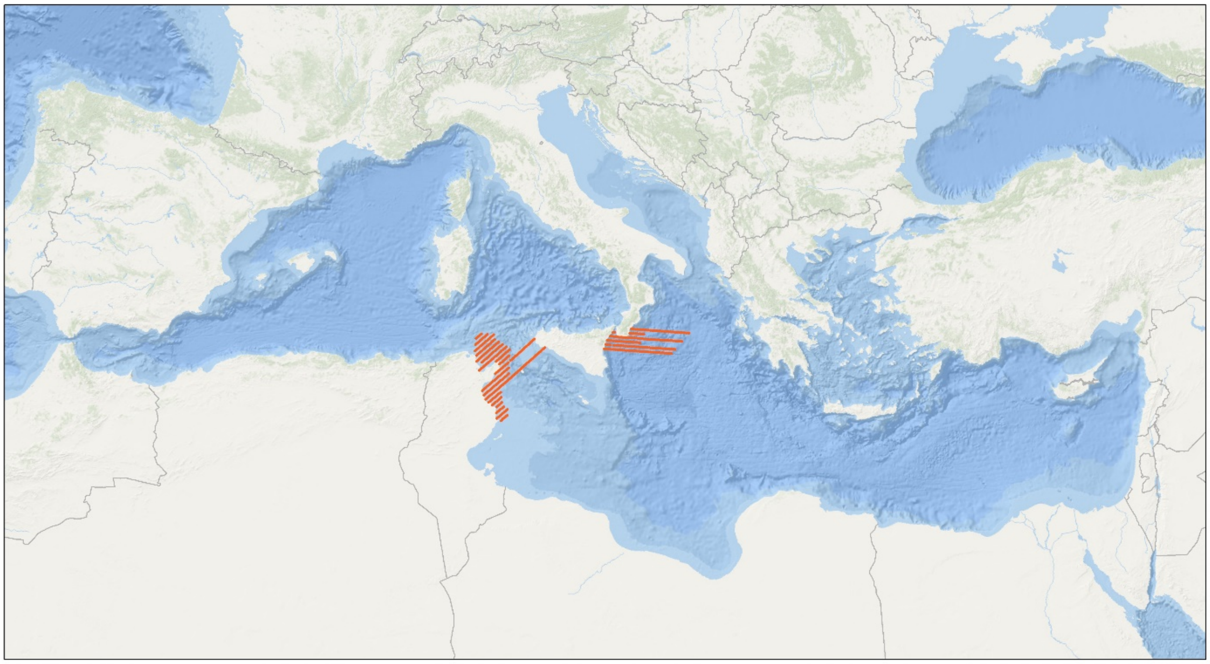

Figure A-4. Available Survey Effort for the Month of April

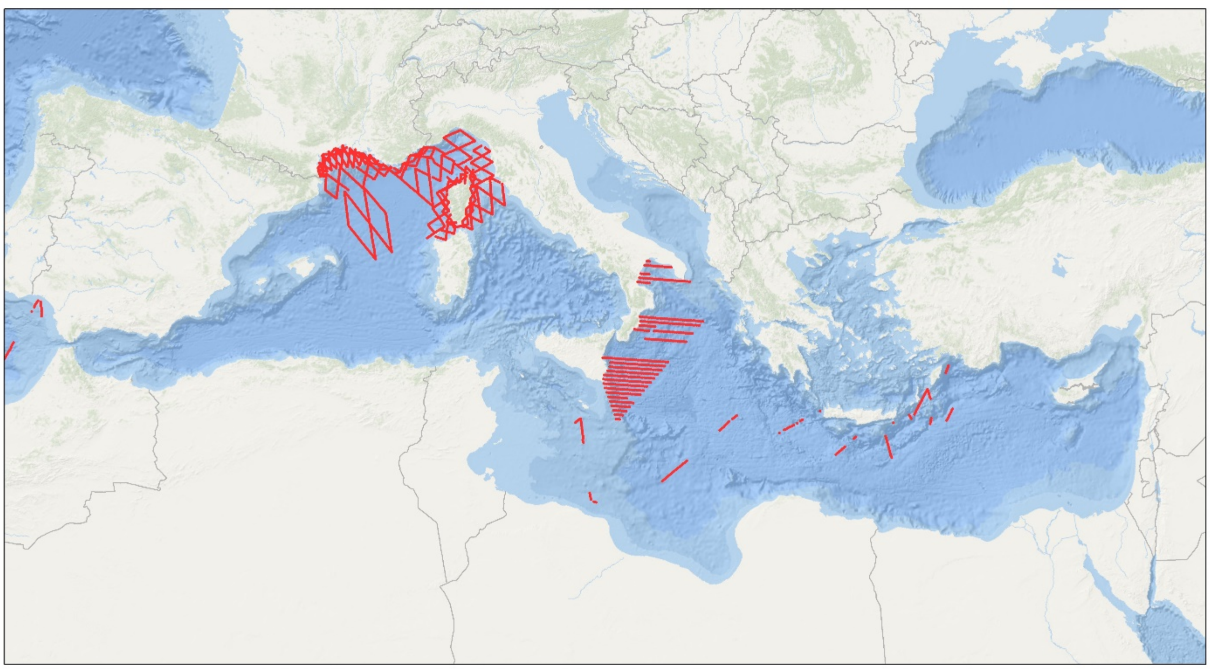

Figure A-5. Available Survey Effort for the Month of May

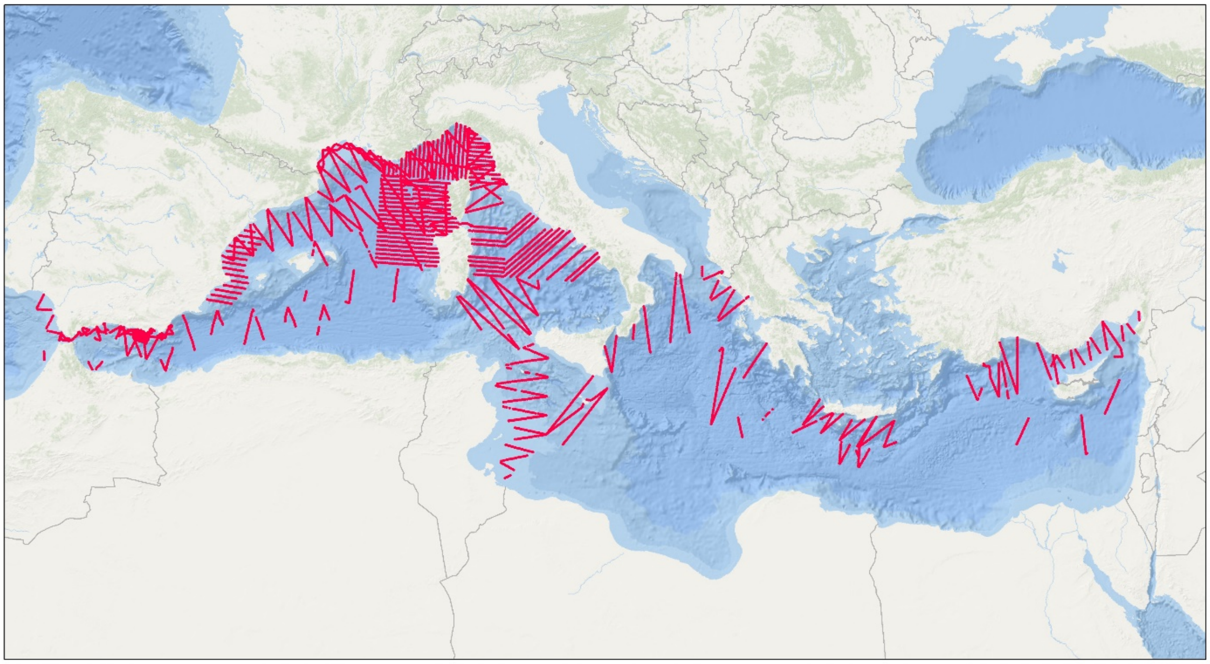

Figure A-6. Available Survey Effort for the Month of June

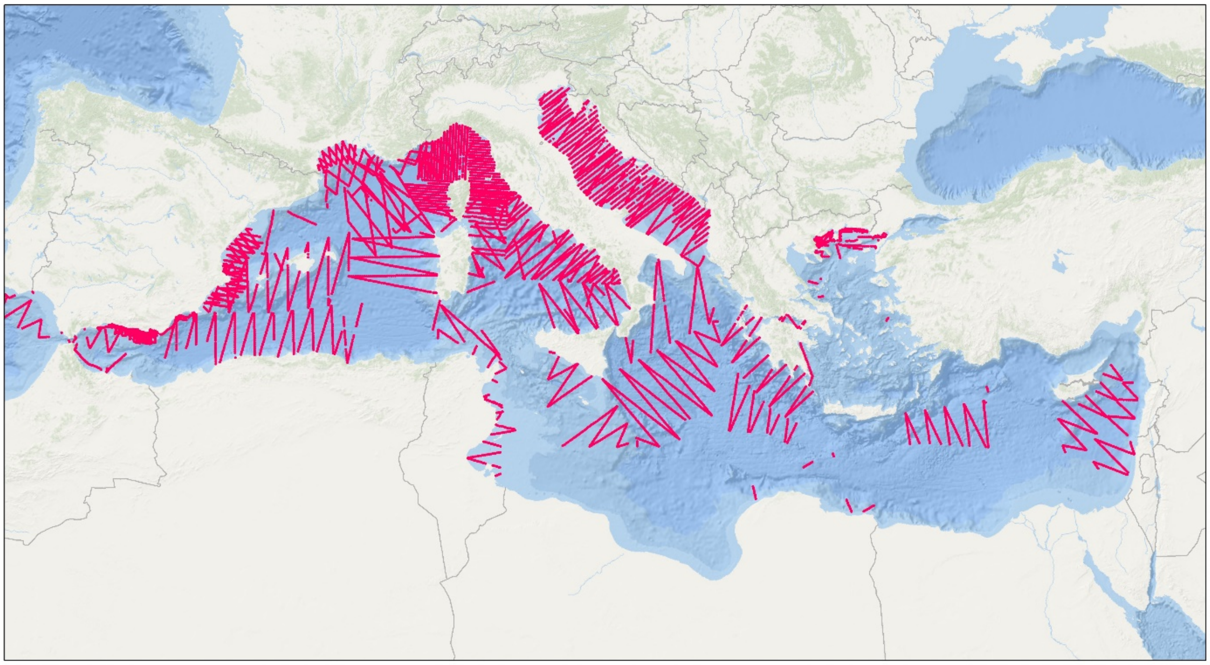

Figure A-7. Available Survey Effort for the Month of July

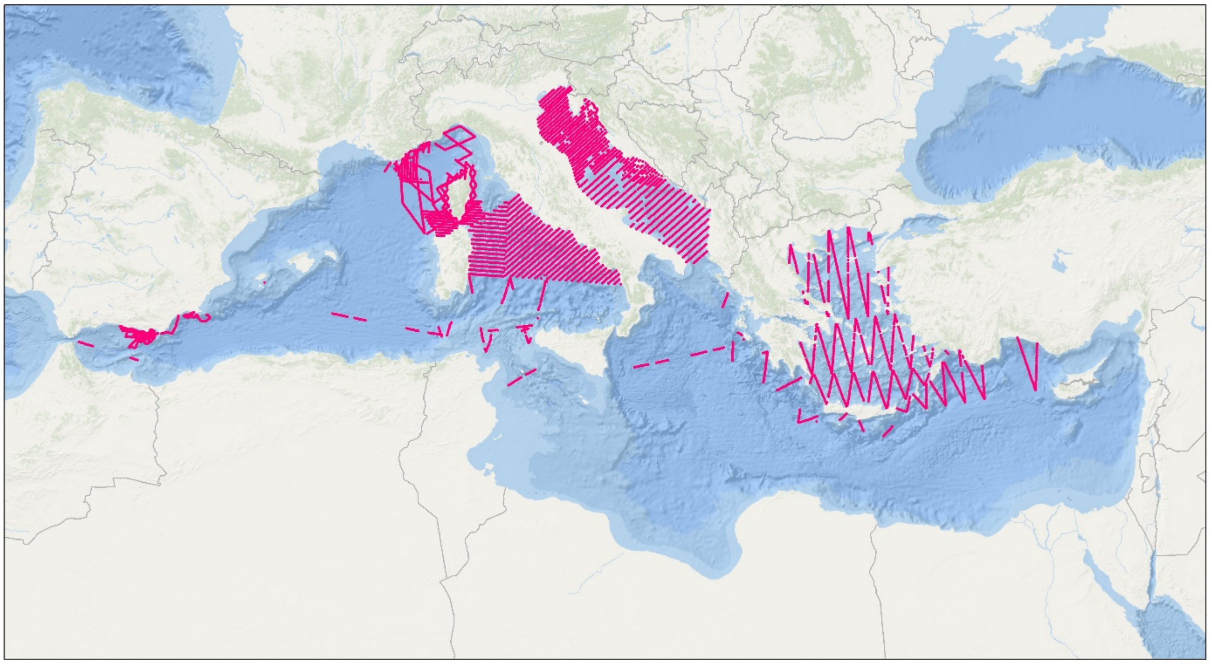

Figure A-8. Available Survey Effort for the Month of August

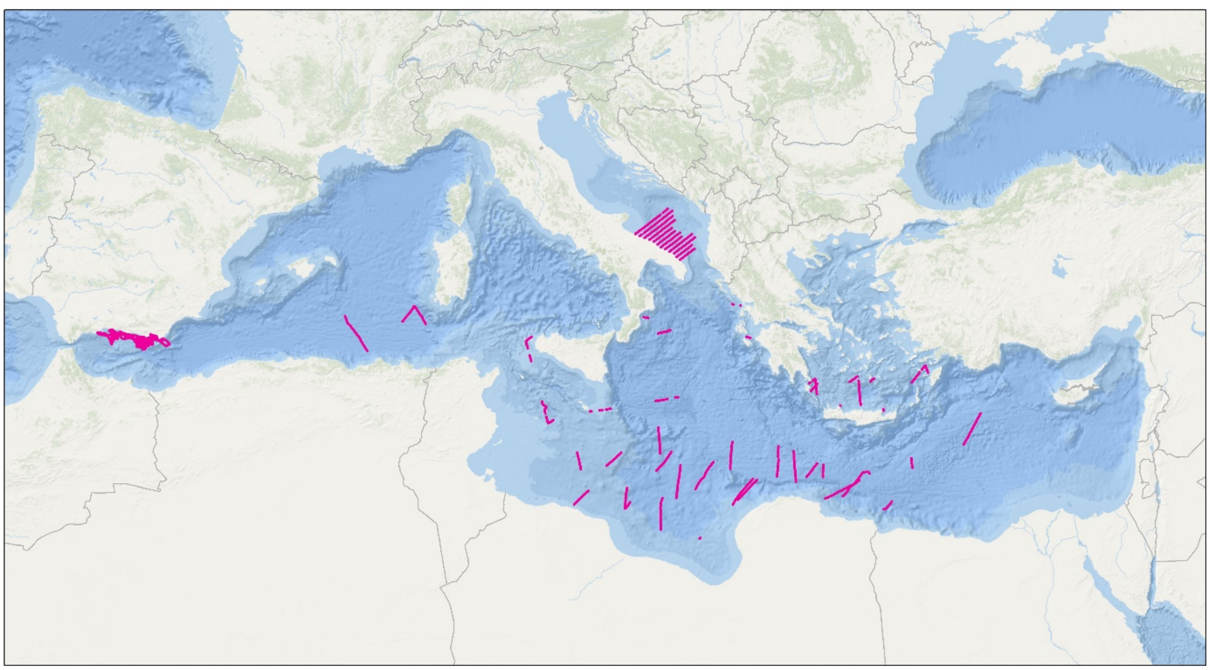

Figure A-9. Available Survey Effort for the Month of September

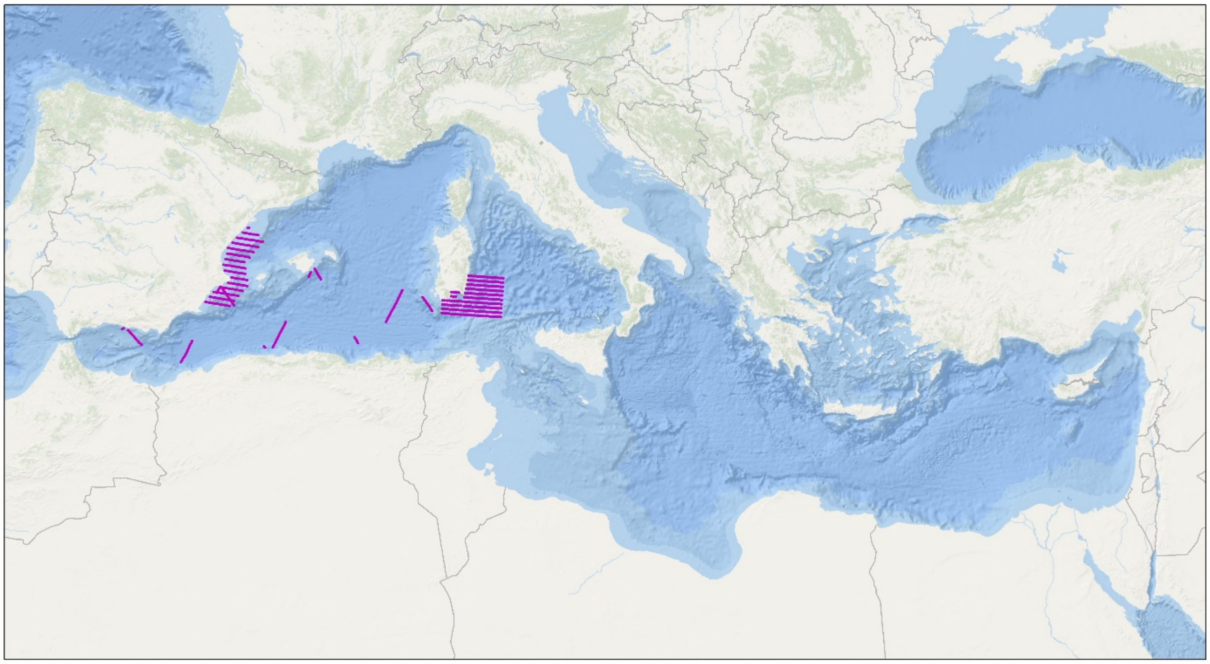

Figure A-10. Available Survey Effort for the Month of October

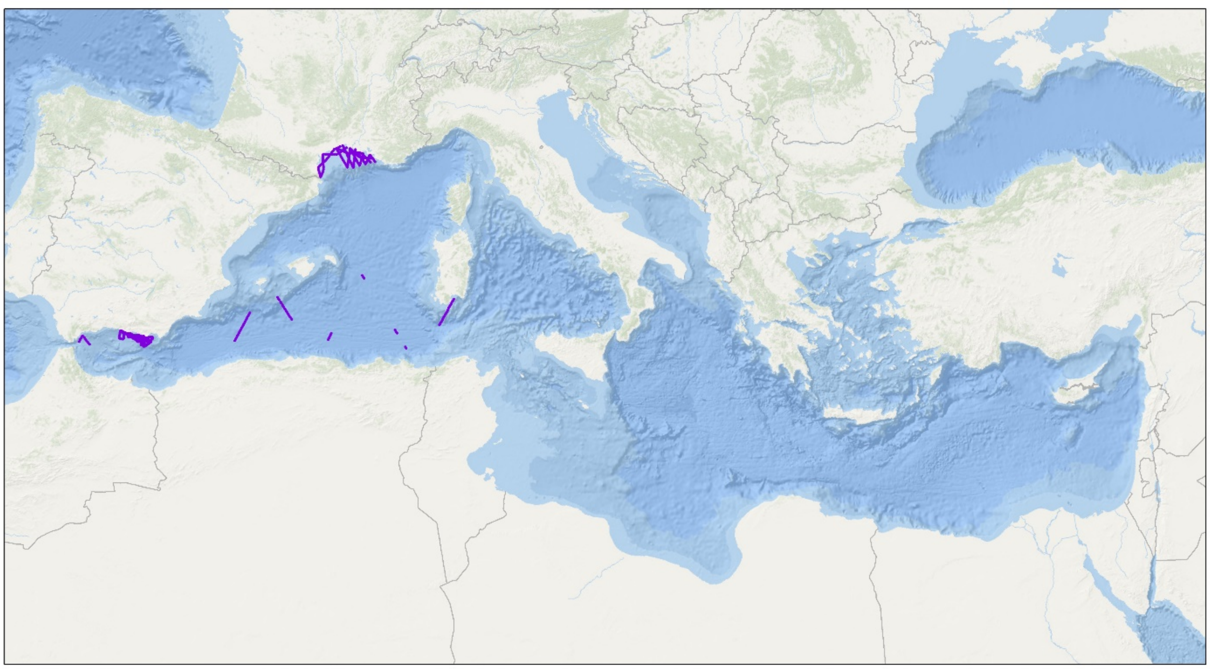

Figure A-11. Available Survey Effort for the Month of November

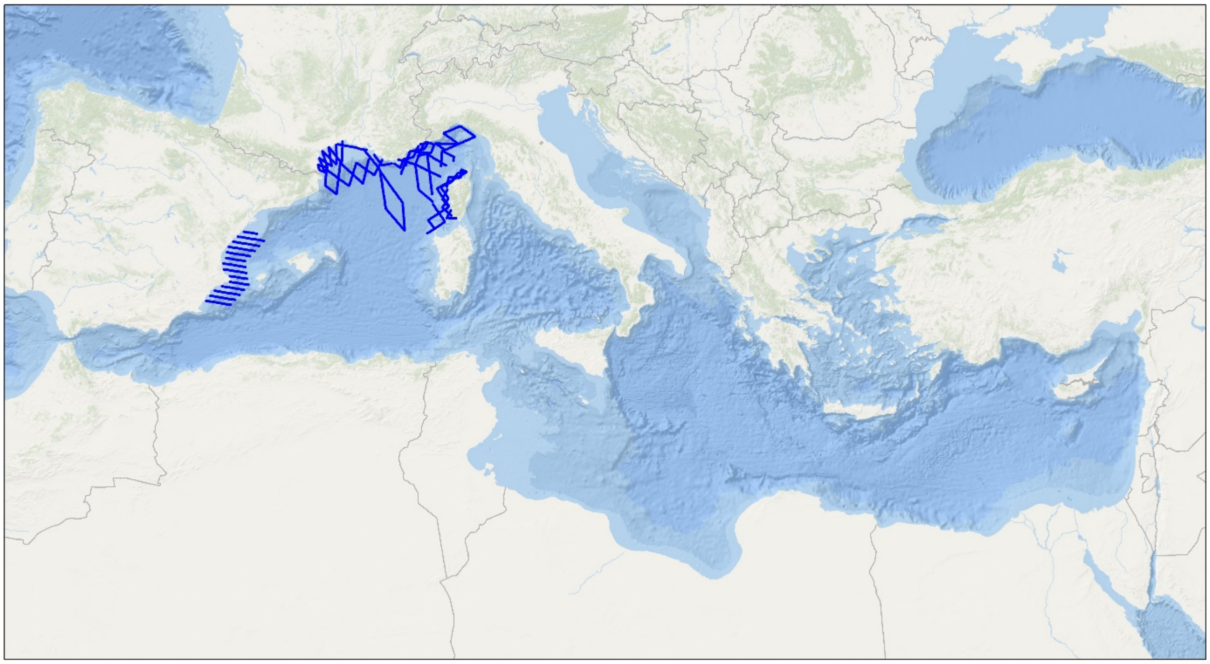

Figure A-12. Available Survey Effort for the Month of December

DISTRIBUTION LIST

External
Defense Technical Information Center

Internal
Code: 1033 (Corporate Research and Information Center)

Total: 2